SEMANTIC

end-to-end Slicing and data-drivEn autoMAtion of Next generation cellular neTworks with mobIle edge Clouds

Marie Skłodowska-Curie Actions (MSCA)
Innovative Training Networks (ITN)
H2020-MSCA-ITN-2019
861165 – SEMANTIC

WP1 – Spectrum and Forward-Compatibility Aspects for multi-GHz NR operation

D1.2: Future-proof NR techniques beyond 5G (M36)

Contractual Date of Delivery:	M36
Actual Date of Delivery:	28/12/2022
Responsible Beneficiary:	CLM
Contributing beneficiaries:	UOA, CLM, NI, FOG
Security:	Public
Nature:	Report
Version:	V1.0

Document Information

Version Date: 28/12/2022
Total Number of Pages: 50

Authors

Name	Organization	Email
Dr. Nikos Passas	UOA	passas@di.uoa.gr
Ayham Alyosef	UOA	aalyosef@di.uoa.gr
Azadeh Tabeshnezhad	CLM	azadeh.tabeshnezhad@chalmers.se
Mehdi Sattari	CLM	mehdi.sattari@chalmers.se
Prof. Tommy Svensson	CLM	tommy.svensson@chalmers.se
Dr. Abdo Gaber	NI	abdo.gaber@ni.com
Muhammad Qurratulain Khan	NI	muhammad.qurratulain.khan@ni.com
Dr. Dionysis Xenakis	FOG	dionysis@fogus.gr

Document History

Revision	Date	Modification	Contact Person
V0.1	04/10/2022	Defining a preliminary table of contents	Prof. Tommy Svensson
V0.2	04/10/2022	Updated Authors	Prof. Tommy Svensson
V0.3	22/12/2022	First complete version	Prof. Tommy Svensson
V0.4	23/12/2022	Polished version	Prof. Tommy Svensson
V0.5	23/12/2022	Update list of Acronyms and Abbreviations	Dr. Abdo Gaber
V0.6	23/12/2022	Minor typos and layout corrected, added Fig. 1	Dr. Abdo Gaber
V1.0	28/12/2022	Final version	Prof. Tommy Svensson

TABLE OF CONTENTS

List of Acronyms and Abbreviations

Abbreviation	Explanation
3GPP	3rd generation partnership project
5G	5th generation of wireless networks
6G	6th generation of wireless networks
ADC	Analogue to digital converter
AF	Amplify-and-forward
AOA	Angle of arrival
BN	Batch normalization
BM	beam management
BS	Base station
CCDF	Complementary cumulative density function
CLM	Chalmers University of Technology
CNN	Convolutional neural network
CSI	Channel state information
DMRS	Demodulation Reference Signal
DNN	Deep neural network
DL	Downlink
DQN	Deep Q-network
DRL	Deep RL
EM	Electromagnetic
ESR	Early-stage researcher
FD	Full duplex
FHPPP	Finite homogeneous PPP
GA	Genetic algorithm
GPS	Global positioning system
IAB	Integrated access and backhaul
IOT	Internet of things
IRA	Integrated resource allocation
KNN	K-nearest neighbors
LDPC	Low-density parity-check
LS	Least square
LSTM	Long short-term memory
MAB	Multi-armed bandit
MBS	Macro BS
MIMO	Multiple-input multiple-output
ML	Machine learning
mmWave	Millimeter-wave communications
MU-MIMO	Multi-user multiple-input multiple-output
MWM	Maximum weighted matching
NI	National Instruments Corporation
NLOS	Non-line-of-sight

NN	Neural network
NOMA	Non-orthogonal multiple access
NR	New radio
OFDM	Orthogonal frequency-division multiplexing
OFDMA	Orthogonal frequency division multiple access
ORA	Orthogonal resource allocation
OMA	Orthogonal multiple access
PBCH	Physical broadcast channel
PD-NOMA	Power-domain NOMA
PPP	Poisson point process
PRACH	Physical random-access channel
PSS	Primary synchronization sequence
QoS	Quality of Service
ReLU	Rectified linear units
RF	Radio frequency
RIS	Reconfigurable intelligent
RL	Reinforcement learning
RNN	Recurrent neural network
RSRP	Reference signal received power
SBS	Small BS
SCA	Successive convex approximation
SI	Self-interference
SIC	Successive interference cancellation
SINR	Signal-to-interference-plus-noise ratio
SISO	Single-input single-output
SL	Supervised learning
SNR	Signal to noise ratio
SRS	Sounding reference signal
SSB	Synchronization sequence blocks
SSS	Secondary synchronization sequence
SVM	Support vector machines
UCB	Upper confidence bound
UE	User equipment
UL	Uplink
ULA	Uniform linear array
UOA	National and Kapodistrian University of Athens
UPN	User provided network
V2X	Vehicle-to-everything
WP1	Work package 1

Table of Figures

Executive summary

This report includes the SEMANTIC ESR contributions towards the objectives of WP1 (Spectrum and Forward-Compatibility Aspects for multi-GHz NR operation).

More specifically, it summarizes the key findings and preliminary performance evaluation results of the ESRs in Task 1.2 Design of 5G and beyond transmission techniques, with a focus on beam-based transmissions in multi-GHz bands; low-complexity techniques for channel estimation in massive MIMO in the mmWave band; distributed MIMO with focus on IAB; and NOMA for enhancing user experience in beyond 5G systems.

Outcomes of this deliverable will be circulated to WP4 to convey to the respective ESRs a list of PHY components, resources and techniques towards the automated control and parameterization of the 3GPP 5G and Beyond (6G) NR evolution.

1 Introduction

One of the key distinguishing features of 5G new radio (NR) is the utilization of high available bandwidth at higher frequency millimeter-wave (mmWave) bands [GPR+19]. To meet even higher throughput requirements, 6G is expected to stretch these spectrum boundaries towards higher mmWave and THz bands [TSM+21]. However, the benefits of higher frequency bands come at the cost of higher propagation loss and severe channel intermittency. These impairments can be compensated by beamforming. To establish high directional links between base station (BS) and user equipment, 5G relies on a set of procedures known as beam management (BM). For initial access during BM, both BS and user equipment (UE) perform an exhaustive beam scan. However, large size codebooks at higher frequencies complicate the exhaustive beam scan-based BM. Machine learning is very well known to deal with complex problems in computer vision and more recently in wireless communications. Thus, in the following chapters, we provide a comprehensive overview of some existing machine learning (ML)-based solution for mmWave BM. We then identify some key challenges for ML-based BM at higher frequencies that might lead to a bottleneck for future wireless communication networks.

mmWave massive multiple-input multiple-output (MIMO) is now a reality but there is still room to boost the capacity of this technology by utilizing new techniques. One of the promising techniques that can be combined by mmWave massive MIMO technology is full-duplex (FD) transmissions. Compared to half-duplex systems, FD transmissions can offer possibly higher data rate and lower latency, making it an exciting opportunity to further improve the capability of mmWave massive MIMO technology. Enabling FD transmissions is hindered by self-interference (SI) that occurs at receive antennas of FD systems. To overcome this interference, SI channel estimation is a crucial step to make FD systems feasible. There are already several challenges such as high pilot overhead, pilot contamination, etc. in channel estimation of mmWave massive MIMO systems, and due to the urge of SI channel estimation, utilizing FD transmissions will further complicate the channel estimation problem in FD mmWave massive MIMO systems. Here, we tackle the problem of channel estimation in FD mmWave massive MIMO systems and several approaches are proposed to reduce the pilot overhead using deep neural networks (DNNs). In particular, we propose to share pilot resources between users and transmit antennas at the BS, in order to have the same pilot overhead as in half-duplex systems.

The dense deployments of mmWave in 5G NR and B5G systems are required to solve problems of sensitivity to link blockage and high propagation losses logically. Some challenges in these deployments are cost-efficient backhauling and difficulties to provide traditional fiber-backhaul access to each cell site [CGG+21]. On the other hand, mmWave communication is proper for both access and backhaul links, so the third generation partnership project 3GPP has recently proposed the concept of integrated access and backhaul (IAB) architecture for the 5G cellular networks in which the same spectral resources and infrastructure will be used for both backhaul and access to reduce the deployment costs by enabling mmWave wireless backhaul connection, where the traffic of the connected users is relayed wirelessly by the IAB nodes in the same mmWave licensed spectrum back to the donor nodes (which is connected to fiber) over one or more backhaul hops. Thus, IAB deployments provides a promising solution in the future wireless networks to accomplish superior cell edge coverage and significantly reduce the amount of required fiber [LVV+20]. The deployment of IAB in a cellular network is cost effective and has the ability of achieving high data rate of about 100 Mb/s with limited fiber connectivity. IAB deployment is not only costly effective, but also time effective, since fiber trenching and permitting is a time-consuming process.

The rapid development of the Internet of things (IoT), multimedia application, and vehicle-to-everything (V2X) communications have led to an increase in the number of UEs, and the need for enhanced data rates for 5G and beyond mobile wireless networks [SMO+19]. To address these demands of massive connectivity, several potential candidate technologies have been proposed, including massive MIMO [BDE+19], ultra-dense networks [XZC+20], mmWave communications [SCW+19], and non-orthogonal multiple access (NOMA) [DSL+17]. All of these techniques are useful for enabling massive connectivity among many wireless devices. NOMA is of particular interest because it allows multiple users to share the same orthogonal time-, frequency-, spatial- and code-domain resource blocks [DWD+18]. In [IAD+16] NOMA was shown to give an improvement in system throughput and user-fairness for a single-input single-output (SISO) channel compared to the orthogonal frequency division multiple access (OFDMA). Since then, many researchers have investigated the benefits of NOMA for next-generation radio access techniques. On the other hand, reconfigurable intelligent surface (RIS) has emerged as a unique technology for improving the spectrum and energy efficiency. RIS consists of large numbers of reflecting elements so it can reduce the number of antennas at the transmitters and receivers for the conventional MIMO NOMA design. Since RIS can reflect electromagnetic (EM) waves, RIS supports FD and full-band transmission. RISs use low power consumption components [YXL+21], [LLM+21].

2 Background on relevant technologies

2.1 Machine Learning based mmWave Beam Management

The wireless communication at higher frequency bands (mmWave and THz bands) suffers from higher propagation loss and severe channel intermittency. To compensate these impairments, beamforming with highly directional transmission links achieved via high dimensional phased antenna arrays is used at the BS and the UE [RPM+21]. Consequently, a precise alignment of beams is required for link establishment. Beam alignment in 5G is achieved through a set of operations known as BM. The BM procedure specified by 3GPP for 5G NR includes initial beam establishment, beam refinement and tracking, and beam failure detection and recovery [GPR+19]. In the following, we provide an overview of the 3GPP specified mmWave BM procedure.

I. Initial Beam Establishment: The first step in the BM procedure is the initial beam establishment during which both BS and UE rely on the exhaustive beam sweeping to select the best beam pair for downlink (DL) and uplink (UL) transmission. To determine a DL beam, pair, the BS transmits the synchronization sequence blocks (SSBs) in all directions at predefined intervals. An SSB is a set of four orthogonal frequency division modulated (OFDM) symbols consisting of primary synchronization sequence (PSS), secondary synchronization sequence (SSS), and the physical broadcast channel (PBCH) with the demodulation and reference signal (DMRS).

   The UE then sweeps all its receive beams to measure the reference signal received power (RSRP) of each SSB and identifies the beam with the highest RSRP. For beam measurement reporting, the UE then transmits the physical random-access channel (PRACH) preamble corresponding to the SS block for which the best beam was identified. The process then ends with the identification of DL beam pair.

   A similar procedure is followed for the determination of UL beam pair, where the UE transmits sounding reference signal (SRS) in UL and the BS measures RSRP of SRSs for identification of UL beam pair. However, the procedure is simplified if beam reciprocity is supported and in that case the DL beam pair can also be used for the UL transmission. Figure 1 shows the exhaustive beam sweeping during initial beam establishment. Table 1 summarizes the initial beam establishment procedure.

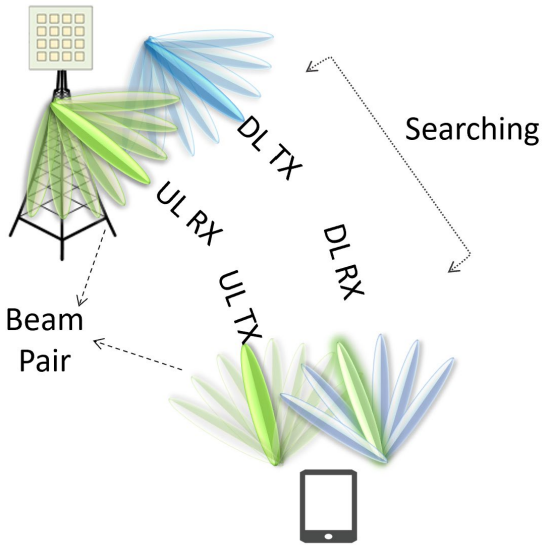

Figure 1: Illustration of exhaustive beam sweeping during initial beam establishment.

Table 1: Summary of initial beam establishment procedure.

Beam Management Phase	Downlink	Uplink
Beam Sweeping	Exhaustive search based on SS blocks received by UE.	Based on SRS (Sounding Reference Signal) transmitted by UE and received by BS.
Beam Measurements	Performed at UE side.	Performed at BS side.
Beam Determination	UE selects best beam based on beam measurements	BS along with central controller selects the best beam pair for communication between itself and UE.
Beam Reporting	UE signals the best beam pair using a PRACH opportunity.	BS signals the best beam pair using an SRS resource indicator.

II. Beam Refinement and Beam Tracking: After establishing the initial connection, the identified beam pair can be further refined during the beam refinement process to establish high directivity. This process focuses on transmit-end beam refinement where the beam sweeping happens at the transmit end by keeping the receive beam fixed. Beam

refinement in the DL is achieved by transmitting SSB or channel state information (CSI)-RS and in the UL is achieved by the transmission of SRS. Second step in the BM process also involves beam tracking that ensures stable link connectivity by updating the beam pairs due to the UE mobility or environmental changes. To enable beam tracking in DL, the UE monitors and compares the RSRP against a predefined threshold and as soon as the RSRP falls below this threshold the UE triggers beam probing to find alternative beam pair.

III. Beam Failure Recovery: Final step in the BM procedure is beam failure detection and recovery. If none of the alternative beams during the beam tracking process offers a better RSRP, a beam failure instance is detected. Once multiple beam failure instances are detected, the UE triggers the beam failure recovery over the PRACH. The BS then responds to this recovery request by identifying new candidate beams for transmission. The Network response to recovery request as a random access response (RAR) as part of contention-free 2-step random access procedure.

To motivate the need for ML based BM, we first highlight some of the key challenges for the existing mmWave BM framework and then provide a comprehensive review of the state-of-the-art ML based studies for mmWave BM.

2.1.1 Challenges for mmWave Beam Management

I. Beam Measurement Overhead: 6G is expected to operate at higher mmWave and THz bands. However, to compensate for the propagation loss at further higher frequencies requires even narrower beams to ensure coverage resulting in large size of the codebook. In the context of the existing BM framework, this means that both the BS and the UE must sweep a huge number of beams for initial beam establishment. Thus, the existing BM framework based on exhaustive beam sweeping will suffer from a huge beam measurement overhead, higher complexity, and higher latency making it non-suitable for low-latency applications.

II. Support for Multiple Antenna Panel: To combat multipath fading and to benefit from diversity, the BS and the UE are usually equipped with multiple antenna panels. As a result, exhaustive beam sweeping needs to be performed over all antenna panels to find the optimal beam which further aggravates the complexity of the existing BM framework.

III. High Mobility Support: Future releases of NR are expected to support use cases with complex mobility patterns and newer applications with

faster rotation and frequent blockage such as virtual reality and augmented reality. Operating at mmWave carrier frequencies, high mobility UEs will experience more frequent handovers. Consequently, application of the existing BM framework with exhaustive beam sweeping is not suitable for highly mobile UEs. Furthermore, high beam training overhead during beam tracking makes the existing BM procedure less robust to high mobility UEs at mmWave bands.

Traditionally, to mitigate the issues of exhaustive beam sweeping a multi-resolution beam codebook is usually utilized at the BS. On this first level the BS scans a smaller set of wider (parent) beams and then on the second level it limits the narrow (child) beam search scan to the best parent beam. In this way hierarchical beam scan reduces the beam sweeping overhead. However, the complexity of multi-resolution beam codebook is still higher for multiple antenna panels and for narrower beams at higher mmWave and THz bands. All these limitations necessitate the need of an enhanced BM framework that avoids the issues of exhaustive beam sweeping and scales well to higher frequencies, multiple antenna panels, and to highly mobile UEs.

Inspired by the successful application of ML in natural language processing and computer vision [KLA21], ML has also been harnessed in wireless communications [HCN+21, KKI+21]. Compared to traditional mathematical modeling-based methods, ML based models enjoy several key advantages. Firstly, traditional mathematical models usually rely on idealized assumptions and may not represent the system accurately. ML models, on the other hand, can model the system's non-linearity and thus can represent it perfectly. Secondly, ML models are highly capable of capturing the high-dimensional features of the propagation environment, such as mobility patterns and blockage locations. Based on these motivations, ML has widely been researched for several aspects of wireless communications including beam management [AHS+22, DA22]. In the following, we provide a comprehensive review of ML based BM approaches.

2.1.2 State of the Art Machine Learning based Beam Management Solutions

To reduce the complexity and increase the robustness of mmWave BM against above mentioned issues, ML has been identified as a key tool that can induce intelligence in the BM framework to better deal with the environmental changes and to avoid the exhaustive beam sweeping. ML based mmWave BM solutions can be categorized into two main classes as: supervised learning (SL) and reinforcement learning (RL) based solution. Based on the availability and utilization of any extra information, SL techniques can be further classified into non-side-information assisted and side-information assisted techniques. In the following, we provide a review of the ML based mmWave BM solution.

2.1.2.1 Non-Side-Information Assisted Supervised Learning

SL is a subcategory of ML that uses labeled dataset to train the model and to yield the desired output. The training dataset includes inputs and corresponding correct outputs which allows the model to learn over time. Accuracy of the model is measured through the loss function and the weights of the model are adjusted until the error has been sufficiently minimized. To achieve minimum error, SL model goes through an extensive offline training. After successful training, the ML model is then used for inference purposes. Some of the common SL algorithms include convolutional neural network (CNN), recurrent neural network (RNN), long short-term memory (LSTM) network, *K*-nearest neighbors (KNN) and support vector machines (SVM). In the following, we sub-categorize non-side-information SL solutions for mmWave BM based on the used ML model.

Neural Network based mmWave Beam Management:

Inspired by human brain, a neural network (NN) is composed of interconnected neurons that learn from their mistakes and improve their accuracy continuously to solve complicated problems. Due to their success in the fields of computer vision, natural language processing, and speech recognition, they have been used to enhance the performance of mmWave BM framework.

A multi-resolution codebook-based BM approach that utilizes a NN to adapt the beam probing codebook for a specific environment was proposed in [HMA21]. The idea here is to train the NN so that the probing beams are directed towards the intended UE. The training data for this purpose consists of the channel vectors between the BS and potential UE. Once the probing codebook is learned, the BS periodically sweeps the learned codebook by transmitting SSBs and the UE reports the received signal power to the BS. The received signal power is then fed into the multi-layer perceptron that identifies a set of candidate beams to try based on the the predicted posterior probability distribution. Through simulation results it was shown that the proposed approach not only reduces the beam sweeping overhead but also achieves a higher signal to noise ratio (SNR) in comparison to traditional multi-resolution codebook-based approach.

CNN is a class of NN that is capable of extracting key features from time series and image data. For this reason, they have widely been used for image related tasks such as image recognition and object classification. Their success in the field of image processing paved their way for application in several aspects of wireless communications including BM. Motivated by the fact that different beam patterns introduce different radio frequency (RF) impairments to the waveform, another mmWave BM approach utilizes a CNN to identify the beams based on their RF fingerprint [PRM21]. This is achieved by providing received I\Q samples

to the CNN that learns to identify the beam IDs based on the identification of the patterns in the I\Q constellation. Through experimental validation it was shown that the proposed approach can predict the actual beam with higher accuracy and without any beam sweeping overhead. Another major contribution of this work is the publication of publicly available dataset [PRM+21].

LSTM based mmWave Beam Management:

LSTM network is a special case of an RNN that is capable of learning long-term dependencies in the input data which makes their application suitable for the BM problem. An angle of arrival (AoA) estimation-based beam tracking approach in [DAM19] uses received signal and previous AoA estimates as an input to the LSTM network which utilizes sequential UE parameters to predict the current AoA. Through simulation results, it has been shown that the LSTM based AoA approach performs better in comparison to traditional Kalman filter based approach. A similar vehicular scenario based mmWave channel tracking approach is proposed in [GWL+19]. Here the LSTM model is used to utilize the past CSI to predict the future channel. To investigate, a multi-input single output system is considered, where the UE is served by multiple coordinating BSs. Channel tracking for this scenario is enabled in two stages. In the first stage, the UE sends uplink pilots to all BSs which estimate the channel to update their beamforming weights. These estimated channels from all BSs are then transmitted to a central LSTM cloud that predicts the channel for the next beam coherence interval. In this way beam tracking overhead is reduced to half. Through simulation results it was shown that the proposed approach not only achieves same transmission rate as achieved by traditional methods, but also reduces the beam tracking overhead to half.

To benefit from the feature extraction of a CNN and to leverage the long-term dependencies in the sequential data, authors in [ECB+21] propose to use convolutional LSTM for mmWave BM. Utilizing the concept of multi-resolution codebook, it was proposed to sweep wider beams in the first step. Beam measurements obtained in the first step are then utilized by CNN that predicts the beam measurements for corresponding narrower beams. In this way beam sweeping overhead is reduced to only wide beam measurements. In the second step, previously obtained wide beam measurements are used by the LSTM model to predict narrow beam measurements for next beam coherence interval. This further reduces the beam sweeping overhead to half for two consecutive beam coherence intervals. Through simulation results it was shown that the proposed approach achieves same transmission rate as traditional methods but also reduces the beam sweeping overhead significantly.

2.1.2.2 Side-Information Assisted Supervised Learning

The main idea behind side-information assisted SL solutions is to use any available side information to reduce beam sweeping overhead. Particularly, an ML model is trained to learn the mapping between the available side information and the suitable mmWave beam. Based on the availability of the side information these solutions can be classified into location assisted and low-frequency CSI assisted mmWave BM techniques.

Location Assisted mmWave Beam Management:

A beam prediction framework that utilizes the location of the UE and the moving objects (vehicles) for environmental perception was proposed in [WNH18]. Once the ML model learns the environment, it can predict the suitable beam based on the location feedback. Similar approaches for vehicular scenario were proposed in [VCS+18, VSB+17]. Both these works consider the availability of UE location but ignores the location availability of other moving objects. Authors in [WKR+19] resolve this issue by considering location awareness of all moving objects for better environmental perception and thus results in better performance. Furthermore, the impact of location inaccuracy was also studied in [WKR+19].

Most of the previous location-based approaches consider vehicular scenario with fixed orientation of the receiver. This is not applicable to pedestrian case, where UE's orientation may change several times even on the same location. To cater for this issue, authors in [RMC20] propose to use UE location and orientation to train the ML model. Once trained, the ML model then predicts probability of the best beam pair. More recently, UE location was used to predict the optimal serving BS and the best candidate beam in [HA+21]. In the first stage, UE feedbacks its location to all neighbouring BSs, where the central ML model then selects the optimal BS among all candidates. In the second stage, UE location is used to determine the optimal beam at the optimal BS. Further, motivated by the promising results of location assisted beam tracking approaches its performance in the real-world scenarios was analysed in [MBP+22]. Here, several ML algorithms that utilize location information were compared and through experimental validation it was shown that the location assisted beam tracking approaches achieve an accuracy of up to 99%.

Low-Frequency CSI Assisted mmWave Beam Management Solutions:

Experimental validations in [HKS18] show that in line-of-sight communication scenarios there exists a correlation between low-frequency and mmWave CSI. This means that low-frequency CSI, which can be achieved with less complexity in comparison to mmWave CSI, can be mapped to mmWave CSI. This fact was

exploited in [SLP+20], where a NN was trained to map the low-frequency CSI to mmWave CSI. In the inference stage, the UE only feedbacks low-frequency CSI and the trained NN can then predict the mmWave CSI to use it for beam prediction purposes. A similar approach in [MZW20] utilizes this low-frequency CSI to train a CNN that predicts the mmWave CSI. The idea was further extended in [MSW21], where instead of instantaneous low-frequency CSI, *L* previously obtained CSIs were used to predict the mmWave CSI. Furthermore, LSTM was used to predict the best beam in between two low-frequency CSI estimation instant. This not only results in better estimate of mmWave CSI but also reduces the beam sweeping overhead.

2.1.2.3 Reinforcement Learning for mmWave Beam Management

RL is a type of machine learning technique that enables an agent to learn in an interactive environment by trial and error using feedback from its own actions and experiences. In contrast to SL, RL is an online learning technique that does not need labelled data for offline training. Because of this online learning capability, RL is suitable for wireless communications due to ever changing nature of wireless communication channel. Based on the type of used algorithm, RL based mmWave BM solutions can be classified into Q-learning and multi-armed bandit approaches.

Q-Learning:

Q-learning is a policy-free RL algorithm that tries to maximize the quality of an action within the current state. It is considered policy-free because the learning agent explores all possible options and maintains a Q-table based on the quality of an action in each state. The Q-table serves as a reference for the agent which then selects the best action based on its Q-value. More specifically, Q-learning seeks to learn a policy that maximizes the total reward.

A Q-learning based BM approach that aims on finding the best beam based on received signal power was proposed in [WOZ+19]. Action space for this problem is the number of beams at the BS, state space is defined as the location of the UE, and reward is based on the received signal power. In any given state the learning agent then tries to select the beam that results in maximum received signal power. During the training phase, it is possible for the agent to select non-optimal beams, but this helps in exploration of alternative beams. Once learning is complete, the agent always selects the best beam resulting in maximum received power. However, based on the size of state-action space, the learning agent usually requires several iterations before convergence, which in the context of beam alignment can result in beam failure.

To overcome the delayed convergence issue of Q-learning, a deep Q-network (DQN) that approximates the quality of actions with the help of a NN is usually used. As a result, DQN achieves lower convergence time in comparison to Q-learning. A DQN based mmWave BM approach that adopts to environmental fluctuations by adjusting the beam search space was proposed in [ZHW+21]. Performance of the DQN based approach was analysed by considering a slow and a fast-moving UE. Through simulation results it was shown that the DQN achieves faster convergence in compassion to Q-learning.

Multi-Armed Bandit:

Multi-armed bandit (MAB) is a category of RL where the agent must select an arm (action) from a set of possible arms that maximizes the long-term cumulative reward. Selecting one action from an action space leads to a well-known explore-exploit dilemma. Several choices of arm selection leads to different approaches that can be used in MAB. Most common approaches to deal with this problem include upper confidence bound (UCB), epsilon greedy, and Thompson sampling.

Initial studies that considered MAB for BM include [HSK+18, WCW+18]. However, in both these proposals each beam was considered as an arm. Intuitively, it can be imagined that exploring each arm (beam) may lead to a scenario where the selected beam has low RSRP resulting in beam failure. To deal with this problem, authors in [HHZ+20] propose to reduce the beam search space by grouping several beams into a single arm. Based on the reduced action space performance of UCB and epsilon greedy algorithms were evaluated, and it was shown that both the algorithms achieve spectral efficiency close to the perfect alignment scenario. Further, to deal with time varying nature of wireless channel use of non-stationary bandit was proposed in [GLS20]. To use the historical information two modified versions of UCB were proposed. The first is called discounted UCB that discounts past observations and assigns more weightage to more recent information. The second approach is the sliding-window UCB that assigns equal weightage to recent information within the size of the sliding window.

Thompson sampling-based MAB for mmWave BM was proposed in [AAF+20]. Here, to achieve enhanced beam alignment accuracy and to achieve higher spectral efficiency MAB was utilized to update the beam in between two consecutive SSB transmissions. Further, to deal with non-stationarity of the wireless environment use of forgetting and boosting factor was proposed. Through experimental validation it was shown that the proposed approach offers higher throughput in comparison to traditional approaches. Main reason for the enhanced throughput is the beam alignment in between consecutive SSBs. The

approach was further studied in [SKA+21], where the use of adaptive forgetting factor was proposed for Thompson sampling-based MAB.

2.1.3 Challenges of Machine Learning based mmWave Beam Management

Though ML based BM solutions significantly reduce the beam sweeping overhead while maintaining or exceeding other performance measures like spectral efficiency and beam alignment accuracy. However, existing ML based mmWave BM solutions suffer from several challenges as discussed below.

In general, a main benefit of integrating ML into BM is its ability to adapt to environmental fluctuations. However, SL based mmWave BM solutions result in good performance once they have gone through extensive training for a specific environment. This means that with the changing environment, the training dataset needs to be renewed and the SL model needs to be retrained with this new data. Consequently, SL based mmWave BM solution solutions are not well generalizable as they are trained and optimized for a specific environment. Side-information assisted SL solutions further suffer from the inaccuracy of the side information. This means that the inaccuracy of the side-information may lead to selection of sub-optimal beam or even to link failure. As a result, methods that are less dependent on the accuracy of the side information are sought. RL techniques overcome the fundamental limitation of SL by offering online learning capability and have found to be quite useful for sequential decision-making problems, but they have slower convergence. Deep RL (DRL) that combines NN with RL has the potential to accelerate convergence. However, DRL has not been well investigated for the BM purposes yet. Therefore, tremendous research efforts are needed to develop a low latent, less complex, and adaptive RL based mmWave BM framework.

Performance of initial beam establishment and beam tracking in the mmWave BM framework is highly dependent on the channel variation due to UE mobility and environmental changes. In all the above surveyed work, performance of the ML model has been evaluated in a specific scenario, which makes it quite challenging to compare these works. Therefore, to compare the performance of ML based BM solutions standardized UE mobility and rotation models are desired. Furthermore, performance of the SL based mmWave BM solutions is highly dependent on the training dataset. However, lack of publicly available standardized dataset for training, validation, and testing is another challenge for ML based mmWave BM solutions.

Operating at higher carrier frequencies, on one hand, results in wider available bandwidths but on the other hand it requires smaller cells to benefit from beamforming. This means that a UE operating at higher frequency bands will

encounter more frequent handovers and might suffer from beam failure due to high mobility. Consequently, BM framework that can support high mobility by utilizing contextual or historical information are sought. Furthermore, all the surveyed works consider BS and UE with single antenna panels. However, to combat fading and to benefit from multi-antenna interference cancellation techniques, it is necessary to consider multiple antenna panels at BS and UE.

To conclude, traditional BM framework, due to its higher complexity and low robustness, might lead to a bottleneck to utilize wider bandwidths at higher mmWave and THz bands for next generation of wireless communication systems. ML can help in developing a BM framework that is suitable for higher frequencies. However, existing ML solutions fail to meet all the requirements of a robust mmWave BM solution, indicating that more research efforts are needed to resolve these problems.

2.2 Channel estimation for full duplex

2.2.1 Introduction and literature review

Current key enabling wireless technologies such as massive MIMO, mmWave communication, ultra-dense networks, etc, have significantly improved the throughput of wireless communication [FRA+14]. mmWave communication can meet high data rate demand thanks to the huge bandwidth that is available in this band and high path loss in these frequencies can be compensated by utilizing the beamforming gain of massive MIMO antennas. Nonetheless, these technologies have only been considered for half-duplex communication and the potential of utilizing FD communication has been overlooked. In FD transmission, a transceiver can simultaneously transmit and receive over the same frequency carrier, thus possibly doubling the spectral efficiency compared to half-duplex systems. Besides, the delay associated with half-duplex transmission would be alleviated in FD systems and this will facilitate meeting low latency requirements for 5G and beyond [APD+14], [LJH+21].

To realize FD transmission, the SI, which is caused by each transmit element onto the entire receive array, has to be cancelled out. Three steps are usually considered for mitigating SI channel effect at the receive antenna arrays: propagation, analogue, and digital domain SI cancellations [LFT+15]. In propagation domain SI cancellation, SI power is suppressed before arriving to the receive chain circuits [APD+14]. In separate-antenna architecture, propagation domain SI cancellation can be achieved by utilizing the path loss between transmit and receive antenna, cross polarization, and antenna conditionality, while a circulator is usually used in the shared antenna architecture to cancel the SI power [APD+14]. Analog domain SI cancellation is performed before the analogue-to-digital-converter (ADC) in the receive analogue chain and digital SI

cancellation further suppress the residual SI power from the propagation and analogue domain SI cancellation in the baseband. The digital domain SI cancellations are capable of suppressing the reflected SI channel from the environment as they utilize SI channel estimates for SI cancellation while propagation and analogue domain SI cancellation can only suppress the direct SI channel. Therefore, in order to achieve accurate digital domain SI cancellation, acquiring SI channel estimates are essential.

Due to large antenna arrays in massive MIMO systems, channel estimation is already an expensive resource-consuming process even in half-duplex systems and requires high pilot overhead. This problem can be further magnified in FD systems due to the essence of obtaining an SI channel which is also a large MIMO channel, making channel estimation a challenging problem for FD systems. Several studies have been conducted for channel estimation in FD systems. In [BAD+12], authors have proposed a pilot-aided channel estimation scheme for a bidirectional communication between a pair of transceivers. A least square (LS) channel estimation scheme has been utilized in [ZZM+17] for a multi pair two-way amplify-and-forward (AF) relaying system. In [XXT+16], an expectation maximization algorithm is exploited for channel estimation problem in the large-scale MIMO system with FD relay. In this paper, authors have considered two different scenarios where in the first one, both BS and relay estimate their respective individual channels, while in the second scenario, only BS estimates the cascaded channel between transmitter-relay-receiver. A two-stage channel estimation approach has been developed in [AT17], where in the first stage, compressed sensing technique is exploited to estimate SI channel. Then, the SI power has been reduced in baseband to avoid saturation and a subspace-based algorithm is employed to estimate residual SI and BS-UE channels. A specific frame structure has been proposed for FD systems and the achievable rate and SI channel estimation have been analysed in [DTM+15]. The effect of periodical calibration period on SI channel estimation has been investigated in [DLM+14]. Authors have analysed how SI channel estimation and separate calibration period can impact the achievable rate.

The main objective of our work is to propose channel estimation schemes that can reduce the high pilot overhead caused by FD and massive MIMO systems. Deep neural networks will be employed to estimate both SI and UE-BS channel. Three different scenarios for SI channel estimation would be investigated. In the first case, UEs and transmit antennas at BS would have orthogonal pilots at different time slots subcarriers. Therefore, UE-BS and SI channels can be estimated without any interference from each other, but the pilot overhead would be extremely high. For the second scenario, only orthogonal pilots will be considered for transmit antennas at BS, and UEs will reuse the same resources for their pilot transmission. Therefore, UEs will create interference for SI channel

estimation but the pilot overhead will be reduced. To further reduce the pilot overhead associated with the large transmit antenna at FD BS, in the third scenario, orthogonal pilots will be assigned only to the UEs, and transmit antenna at BS will reuse the same pilot resource for SI channel estimation. In this case, the pilot overhead for FD systems will be the same as half-duplex ones but acquiring SI channel estimates with fewer pilots than the number of transmit antenna will be a challenge that can be solved with the powerful learning abilities of deep neural networks.

2.3 Integrated backhaul and access

In the development of mobile communication systems, network densification has become as natural evolution to meet the challenges related to the high losses that mmWave links suffering from. So, backhaul link will be the bottleneck of future wireless networks. IAB technology has been introduced in Release 16 in 3GPP specifications as an important new feature in 5G new radio which enables rapid and cost-effective mmWave deployments [MMF+20], to backhaul the data by creating a wireless multihop relay network between nodes, and it has received substantial interest [ZKA21].

In order to accurately characterize the coverage probability of an IAB-enabled cellular network using its downlink rate, the authors in [SAD18] have developed an analytical approach, by creating an analytical framework that is both realistic and manageable to investigate the performance of IAB-enabled mm-wave HetNets. The study has been taken into account a two-tier HetNet with a number of small, low-power cells layered on top of a circular macrocell with anchored BS (ABS) in the center. The macrocell generating hotspots are supposed to have a non-uniform distribution of users, and the small BSs (SBSs) are situated at the geographic centers of these user hotspots. The analysis of this arrangement differs significantly from the most recent Poisson point processes (PPP)-based models due to the non-uniform distribution of the users and the spatial interaction of their locations with those of the SBSs. Additional insights into the coverage zones are made possible by taking into account a single macrocell, which made it possible to conduct a novel analysis of the load placed on ABS and SBSs, with the assumption that the system's total bandwidth is divided into two for access and backhaul communication. Also, the authors utilize this model to examine the effectiveness of three backhaul bandwidth partition schemes. namely: (i) equal partition, where each SBS gets equal share of bandwidth irrespective of its load, (ii) instantaneous load-based partition, where the ABS frequently collects information from the SBSs on their instantaneous loads and partitions the backhaul bandwidth proportional to the instantaneous load on each SBS, and (iii) average load-based partition, where the ABS collects information from the SBSs on their average loads and partitions the backhaul

bandwidth proportional to the average load on each SBS. Simulation results show two important system-level insights: (i) for three performance metrics namely: downlink rate coverage probability, median rate, and 5th percentile rate, the existence of the optimal access-backhaul bandwidth partition splits for which the metrics are maximized, and (ii) maximum total cell-load that can be supported using the IAB architecture.

An analytical model for characterizing the performance of an IAB-enabled HetNet operating in the mm-wave frequencies has been created by Saha and Dhillon [SD19]. The authors assume that only the macro BSs (MBSs) have access to the fiber backhaul while the SBSs are wirelessly backhauled by the MBSs over mmWave links. The rate coverage of the downlink data rate, or alternatively the complementary cumulative density function (CCDF), that a user experiences in this IAB setting has been derived by the authors for two resource partition strategies at the MBS: (a) integrated resource allocation (IRA), where the total bandwidth is dynamically split between access and backhaul, and (b) orthogonal resource allocation (ORA), where a static partition is established for the access and backhaul communications. The analysis clearly shows that offloading users from MBSs to SBSs may not result in rate improvements comparable to those that would be seen in a HetNet with fiber backhauled SBS in an IAB context. Due to the speed constraint on wireless backhaul links between MBS and SBS, the analysis also demonstrated that it is not possible to increase the user rate in an IAB context by only densifying the SBSs. The authors propose a novel approach to incorporate the effects of correlated blocking into the formulation of cell load, which is a crucial component of the rate characterization, despite the fact that it was known that doing so would be difficult to do mathematically and would be unscalable in system-level simulations. The description of the joint distribution of the signal-to-interference-plus-noise ratio (SINR)'s of the access and backhaul links when the average UE associates with the SBS is another significant innovation of this work. Using these results, they derive tractable expressions of rate coverage for both IRA and ORA strategies.

Authors in [LTX20] have analysed the user provided network (UPN) formed under D2D links to study 5G IAB networks, by applying a Nash bargaining problem to encourage equitable cooperation and enhance user resource usage. The UPN service under 5G IAB networks is modelled as two-tier multi-hop, multi-path hybrid mesh networks, and this framework is used to study the UPN service under IAB networks. According to this architecture, each user's utility function, energy loss function, available energy budget, and cost of downloading data are parameterized. For BSs, the interference between backhaul links and resource limitations are taken into consideration. A virtual currency-based payment system is created to encourage user cooperation by providing rewards for users who share their data with others. It is vital to balance the objectives of all users and

the operator in the incentive design and resource allocation design since each user who shared data wants to receive their own maximum compensation and the operator wants to use UPN to increase the efficiency of resource use. In order to do this, a cooperative game based on the Nash bargaining solution is created in order to assess user cooperation fairly. The suggested Nash bargaining problem in this work, however, differs from the pure Nash bargaining problem in that the resource allocation controlled by the BS is also involved in the negotiation process among users to increase resource usage efficiency. In this work a centralized optimization algorithm has been developed, and it is noted that the centralized algorithm requires the operator to compile all pertinent participant data in order to arrive at the best result, raising concerns about participant privacy. Auxiliary variables are integrated with the primal-dual decomposition technique to get around this problem. The fundamental issue is divided into operator and user-specific sub problems. It is demonstrated that the solution of the distributed algorithm converges to the best solution of the centralized method by transferring intermediate parameters back and forth between users and iteratively executing sub problems. With a confidence level set to 90%, simulation results show that in over 300 iterations of instances when the UPN of users over a geographical area of 100m×100m, the performances of Ind. w/ RA and UPN w/o RA are the same. However, the diversity of users influences the access link rate. The first of the three examined cases see an increase in data download using the suggested UPN solution of between 20% and 40%. The second time the users are divided into two groups, one with high link access and the other with limited link access, the outcomes are identical to the first. The third example, however, demonstrate that as users become more diverse, and the proposed UPN solution increases from 7% to 20%. The outcomes demonstrate the effectiveness of the UPN is increasing network throughput. Additionally, the decentralized approach introduced to mitigate the privacy problems introduced by the centralized approach adopted increases the resources expended by the network to converge to an optimal solution. This could reduce the efficiency of the network under dynamic traffic requirements.

The joint optimization of association and resource allocation in terms of subchannel and power for IAB network has been studied by [LLK+21]. By considering a multi-hop backhauling, the authors have addressed the association and resource allocation issues for wireless backhaul and access links. The authors break down the optimization issue for the IAB network into three subproblems which are association, subchannel allocation, and power allocation, and these subproblems are solved alternately to produce a local optimal solution. The backhaul and access links for the association issue are configured using the Lagrangian duality approach. The work employs a low complexity iterative approach based on successive convex approximation (SCA), which reduces the

non-convex problem to a series of convex problems, to solve the subchannel and power allocation problems effectively. The SCA approach has been noted as a technique that ensures convergence to a local optimum. Simulation results show that spectral-efficient association and diversity gain are both achieved by the suggested algorithm. Additionally, the proposed algorithm for the IAB network outperforms the current schemes by permitting the usage of multi-hops backhauling and the offloading of UEs from MBS to SBSs. Through the use of multi-hop backhauling, simulation results show that the proposed method outperforms single-hop backhauling-based networks in terms of performance and improves network capacity and coverage.

Turgut and Gursoy [TG17], have presented an analytical framework to analyse heterogeneous downlink mm-wave cellular networks consisting of *K* tiers of randomly located BSs, where each tier operates in an mm-wave frequency band. SINR coverage probability is derived for the entire network using stochastic geometry tools. The distinguishing features of mm-wave communications, such as directional beamforming, and having different path loss laws for line-of-sight and non-line-of-sight (NLOS) links were incorporated into the coverage analysis by assuming averaged biased-received power association and Nakagami fading. By using the noise-limited assumption for mmWave networks, a simpler expression requiring the computation of only one numerical integral for coverage probability is obtained. Also, the effect of beamforming alignment errors on the coverage probability analysis is investigated to get insight on the performance in practical scenarios. Downlink rate coverage probability is derived as well to get more insights on the performance of the network. Moreover, the effect of deploying low-power smaller cells and the impact of biasing factor on energy efficiency is analysed. Finally, a hybrid cellular network operating in both mm-wave and μ-wave frequency bands is addressed. Numerical results show that mmWave cellular networks can be approximated to be noise limited rather than being interference-limited especially if the number of tiers is small. The authors also show that increasing main lobe gain results in higher SNR coverage. Moreover, they observe the effect of biasing, where the increasing in the biasing factor of smaller cells has led to better coverage probability of smaller cells because of the higher number of UEs connected to them, while the overall network coverage probability has slightly diminished due to association with the BS not offering the strongest average received power. Furthermore, their work shows that smaller cells provide higher rate than larger cells. Additionally, it is verified that there is an optimal biasing factor to achieve the maximum energy efficiency. The effect of alignment error on coverage probability is also quantified. Finally, they have demonstrated that the proposed analytical framework is also applicable to μWave-mmWave hybrid networks and glean interesting insight on the impact of interference when operating in μWave frequency bands.

Topology optimization and routing in IAB networks are the research subject of Madapatha et al. [MMM+21]. The authors create a number of efficient genetic algorithms (GA)-based approaches for this study's implementation, including ones for the distribution of dedicated non-IAB backhaul connections as well as the placement of IAB nodes. They provide the outcomes for the scenarios using a finite homogeneous PPP (FHPPP)-based stochastic geometry model, in this case, focusing on the features of mmWave communications. They take into consideration the network service coverage probability, which is the likelihood that the UEs' minimum data rate needs are reached, as the metric of interest. To avoid both the long-term and the temporal blockages via topology optimization and routing, respectively, the effects of temporal blockages and routing on the coverage probability were also explored. Although as at the time this paper has been published, mesh-based communication is not yet taken into account by 3GPP IAB specification, the setup provided some indications as to its usefulness in IAB networks. This work also has been examined the impact of other factors, including antenna gain, obstruction, and tree foliage, on the functioning of the system in both scenarios of carefully planned and haphazard network deployments. The performance of the GA-based approach has been compared to that of various cutting-edge topology optimization techniques in numerical findings. Additionally, the authors have investigated the effectiveness of deployment optimization in scenarios where the network topology is constrained and IAB nodes and non-IAB backhaul lines cannot be placed anywhere they want.

On the other hand, the authors in [LWS20] have investigated the joint resource allocation and IAB nodes placement problem for a MIMO OFDMA based IAB network, where an optimal (sum-rate maximization) resource allocation algorithm has been developed which considers subcarriers/spatial sub-channels assignment and the associated power allocations. They also provide two low-complexity suboptimal resource allocation schemes for IAB-enabled network, with systematic approaches which determine the optimal node locations according to two propagation models, and another numerical approach is presented to solve the IAB node placement problem, which guarantees mean load balance. The study also involves the channel aging impact, which appears due to the time lag between the estimated time CSI about a hop and transmitted time when signal is transmitted over that hop. Furthermore, it lights the importance of channel prediction where MBS employs a Wiener-type predictor to predict the channel aging effect, based on channel’s time-varying behaviour model, the resource allocation algorithms show with channel aging the centralized resource allocation control can be valid for low-mobility UEs only where time-varying effect is not serious. The advantages of frequency reuse and multi-hop transmission is discussed and they analyse the resulting co-channel

interference to maximize the frequency efficiency. The resource allocation schemes with frequency reuse show better performance than resource allocation scheme without frequency reuse, although the proposed suboptimal resource allocation algorithms only degrade little or barely in terms of sum rate performance, according to numerical results, even if the optimal resource allocation algorithm produces the best performance. Simulations validate the node placement recommendations and demonstrate their efficacy and precision. If the UE distribution and association rule are known, the same approach can be used for many cellular topologies. They demonstrate that, assuming the time-varying effect is not severe, the resource allocation algorithms with channel aging consideration may successfully compensate for the performance loss, limiting the use of centralized resource allocation control to low-mobility UEs.

A semi-centralized resource allocation scheme, compliant with the 3GPP IAB specifications for IAB networks, flexible, with low complexity has been proposed by [PZP+22] to solve interference and capacity sharing issues resulting from the multiplexing of different links in the same frequency bands, for use in IAB networks for 5G and beyond. The authors demonstrate that the addition of the resource allocation collaboration significantly increase the system's end-to-end throughput and delay, eliminating (or at least limiting) the resurgence of network congestion on the backhaul links. The results show providing up to a 3-fold increase in worst-case throughput and roughly a 30% reduced worst-case latency. The authors discuss the factors to take into account when deploying a semi-centralized resource allocation controller in the real world. The authors specifically address the fact that the proposed approach is predicated on the idea that IAB-nodes can exchange timely feedback information with the IAB-donor. This work develops a generic optimization algorithm, which optimize a certain utility function that is selected with a configurable periodicity in the access and backhaul splitting. The proposed framework subdivides into the following phases, which are periodically repeated: Initial setup phase, which consists in the computation of the simplified IAB network graph and contains active cell associations, then the information collection phase, where the IAB-nodes send information for each of their children nodes to the central controller (e.g. load, available capacity and channel quality). Then centralized scheduling indication phase: once the information received at the central controller it updates the set of weights and maximum weighted matching (MWM) is computed, then it decides the children with the highest priority to be served by their parent nodes firstly, then, these scheduling indications move to the parents IAB-nodes to act accordantly. Finally, a distributed scheduling allocation phase is implemented, last phase of the resource allocation procedure, where IAB-nodes get benefit from the indications received by the central controller to achieve the actual scheduling (which is predominantly distributed), serving the highest priority nodes

first. Additionally, the work contend that this approach is a significant constraint despite the fact that the proposed approach only requires a small amount of signalling data and performs well even when the central allocation period is extended. Furthermore, the unfavourable mmWave propagation characteristics made this disadvantage worse. As a result, the authors have been implemented proposed solutions incorporating a central controller that depend on the reliable and timely interchange of control information with the IAB-donor would likely need dedicated control channels, possibly at sub-6 GHz, in order to give the feedback information, the highest priority. This delineate that the framework could significantly improve the performance of IAB networks, even though its implementation in 5G and future deployments would require more research.

To conclude, there have been several studies on the performance of IAB networks with many research aspects, e.g., optimal node placement, resource allocation and routing, joint node placement and resource allocation scheme, IAB deployments in network densification, the coverage probability of IAB-enabled mmWave and multi-hop topology. Actually, the optimum performance of IAB networks requires accurate deployment of BSs in order to achieve better network load balancing. Stochastic geometry and point processes are good to determine the best cells deployment and network topology and to evaluate the coverage probability and several bandwidth allocation schemes of mmWave-enabled IAB heterogeneous networks.; where many stochastic geometry algorithms were proposed to solve IAB deployment problems like [SGM17], [TG17], [SKG+15], [SAD18], [SD19]. Yet, there is no work providing the high fairness in coverage and resources allocation in the backhaul links for all network nodes especially the down-streaming nodes, which requires novel and deterministic approaches that combine several resource allocations schemes, strategies and high dynamics network topology, which could guarantee the best solutions in such joint optimization problems.

2.4 Non-orthogonal multiple access

NOMA is an interesting technique since it enables multiple access of many users in the same resource, and generally, is divided into two main classes: power-domain and code-domain [SZS+18]. Power-domain NOMA (PD-NOMA) exploits situations where the users have different power levels. As Figure 2 illustrates, in downlink of power-domain NOMA, the users nearer to the BS have better channel conditions compared to distant users who require higher transmission power to mitigate the higher path loss. The idea behind power-domain NOMA is that the users nearer the BS can employ successive interference cancelation (SIC) to remove the strong signal destined for the remote users before decoding their own signal [TJ91].

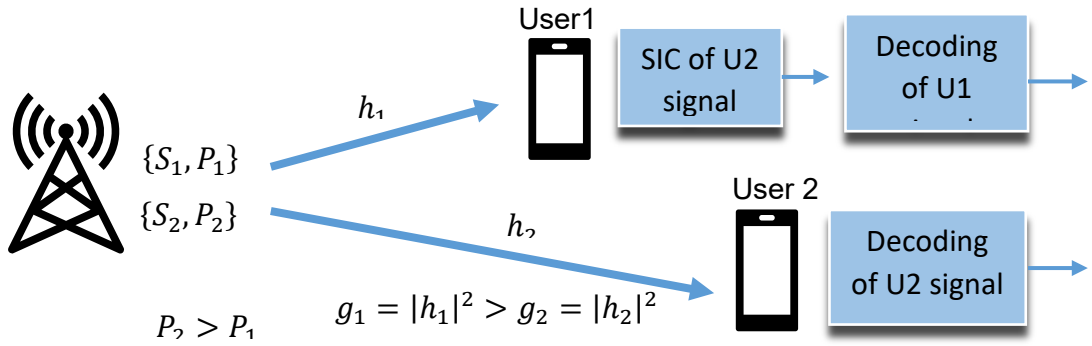

Figure 2: Illustration of Downlink of Power-domain NOMA.

In the uplink power-domain NOMA, as Figure 3 illustrates, the SIC is implemented at the receiver of the BS. In the first step, the receiver decodes the signal of near user that has a better channel condition, it subtracts it from the received signal to decode the signal of far user [YYA+13].

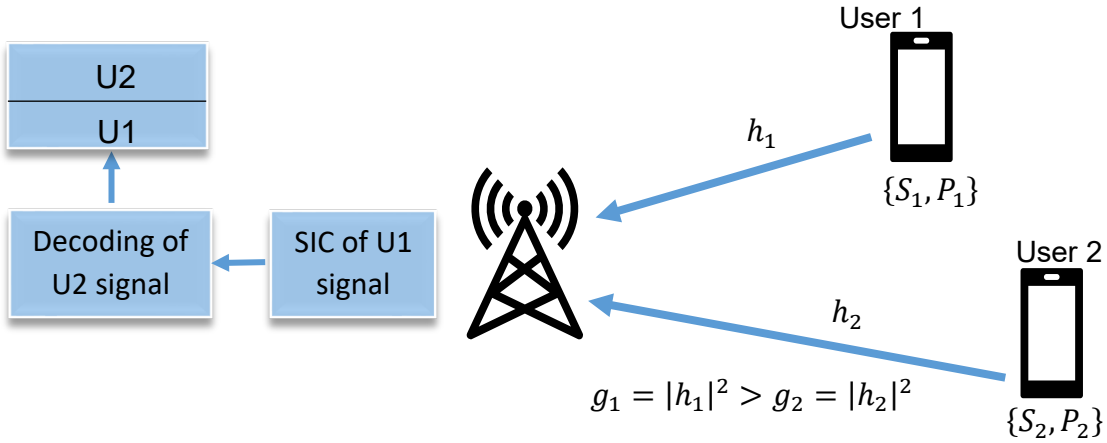

Figure 3: Illustration of Uplink of Power-domain NOMA.

In code-domain NOMA, random Gaussian codes are used at the transmitter in order to maximize the users' detection probability and to minimize symbol error rates [YYA+13]. The superiority of NOMA over conventional orthogonal multiple access (OMA) techniques is derived from the improved spectral efficiency due to the sharing of time/frequency/space/code resources, its allocation of different Quality of Service (QoS) levels to users based on power level allocation, and the fact that it supports massive connectivity, lower latency and an enhanced cell-edge user experience [IZD17].

3 Methodological Tools

3.1 Simulation Tools at UOA

3.1.1 MATLAB

MATLAB can be used to test mathematical models with deferent scenarios. MATLAB has the required toolbox to simulate under various scenarios, so MATLAB can be used for modelling the proposed mathematical node connectivity matrix, modelling the proposed algorithms, and to proof that the mathematical and simulated model are in agreement. System and channel model simulation on MATLAB can be used as a proof of concept after achieving the required mathematical model. MATLAB is used to trouble shoot the working model under various scenarios before actualizing a physical working prototype or system.

3.2 Simulation Tools at NI

With the completion of our literature review, we did some initial exploration to select a suitable tool for our simulation setup. The exploration was based on the required capabilities for traditional BM and ML.

3.2.1 MATLAB

To develop a traditional BM framework, signal processing capabilities at both physical and medium access control layer are required. These capabilities are very well provided by MATLAB. To cover various signal processing capabilities MATLAB provides several toolboxes. Furthermore, the support for ML was also added in the recent releases of MATLAB through their deep learning toolbox. However, here it is worth mentioning that MATLAB is a proprietary simulation tool, and one must pay a huge cost to benefit from various toolboxes of MATLAB.

3.2.2 Python based Libraires

In comparison to MATLAB, Python is an open-source programming language and is free to use. Most popular Python based libraries that provide ML capabilities include PyTorch and TensorFlow. Both these libraries provide comprehensive ML capabilities and include most recent ML models. However, these libraries do not provide much of signal processing capabilities. Thus, a simulation tool that provides simulation abilities of ML and signal processing is needed.

3.2.3 SIONNA

To bridge the gap between signal processing and ML capabilities, recently NVIDIA launched a link level simulator called SIONNA. It is a GPU based open

source library that enables rapid prototyping of complex communication system architectures and provides native support for the integration of machine learning in 6G signal processing. It supports a growing set of features, such as multi-user multiple-input multiple-output (MU-MIMO) link-level simulations with 5G-compliant low-density parity-check (LDPC) and Polar codes, 5G channel models, OFDM, channel estimation, and additional ML capabilities. However, as SIONNA was launched recently in 2022, some of the signal processing capabilities like reference signalling and synchronization are still missing in the current release.

As a result, we will use MATLAB in combination with Python. Due to the availability of signal processing capabilities in MATLAB, we will be able to develop the simulation environment faster. For deep learning, we will use MATLAB with python.

3.3 Simulation Tools at CLM

3.3.1 Deep learning-based channel estimation

Deep learning is a sub-field of machine learning that has been recently utilized in variety of problems in wireless communications including channel estimation. To estimate channel for different scenarios that have been introduced in the section 2.2.3, we employ CNNs. The diagram of the CNNs is depicted in Figure 4.

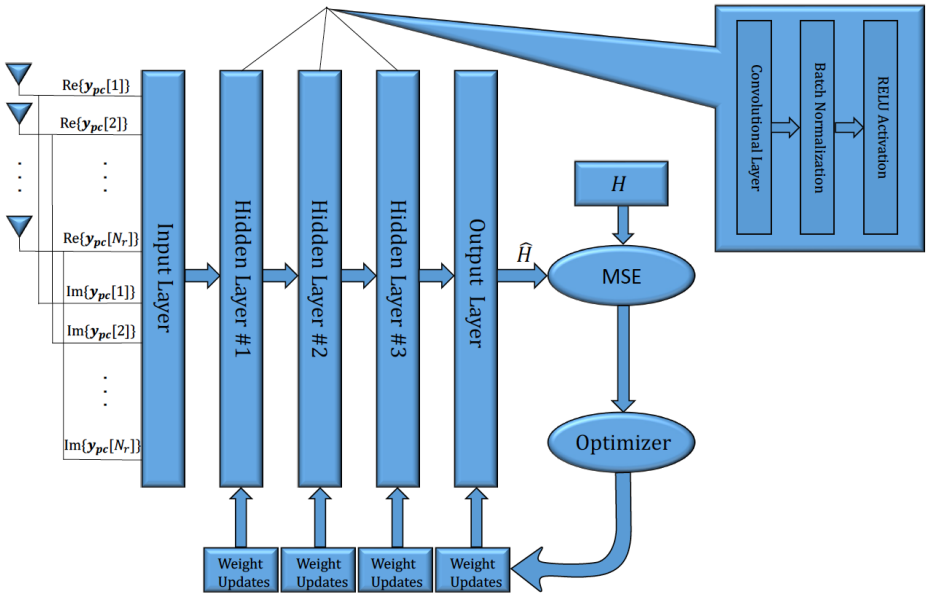

Figure 4: Architecture of deep neural network.

The input of the CNNs is the correlated received pilot signal with the corresponding transmitted pilot signal, either pilot signals of BS or UE, i.e., $\boldsymbol{Y_{pc}} =$

$\boldsymbol{Y_p} * \boldsymbol{X_p^*}$ and the output is the estimated channel. Since tensors do not support complex operations, the input and output dimensions are $\boldsymbol{N_r} \times \boldsymbol{T} \times \boldsymbol{2}$ and $\boldsymbol{N_r} \times \boldsymbol{N_T} \times \boldsymbol{2}$ for SI channel, and $\boldsymbol{N_r} \times \boldsymbol{K} \times \boldsymbol{2}$ for UE-BS channel respectively, where the real and imaginary parts of received correlated pilot signal and estimated channel are put into the third dimension of tensors. After each convolutional layer, a batch normalization (BN) layer is added to increase the stability of learning DNN and avoid vanishing gradients. Then, rectified linear units (ReLU) and linear activation functions are applied for hidden layers and output layers, respectively.

3.3.2 MATLAB

We have solved an optimization problem that the objective function and constraints are both non-linear and non-convex. We used *fmincon* in MATLAB that is a non-linear programming solver. *fmincon* is a nonlinear constrained optimization solver that supports both non-linear and linear constraints. *fmincon* finds a constrained minimum of a scalar function of several variables starting at an initial estimate. This solver is only available if the optimization toolbox is included in your MATLAB installation.

4 Research progress and next steps

4.1 Machine Learning based mmWave Beam Management

In this section, we provide a summary of research progress and specify our next steps. Here, we would like to mention that the NI-1 ESR joined the project at a later stage in February 2022. Hence, the summary of the literature review along with initial exploration of simulation tools has been provided in this deliverable.

4.1.1 Current Status and Results

During this period, we first studied the 3GPP specified BM framework for 5G NR and then studied some of the traditional methods to overcome its limitations. We then started reviewing ML based BM techniques and learned how ML can help mitigating the limitation of the existing BM framework. We researched on different types of ML algorithms that have been used for the BM problem. As specified in the previous sections, we found that ML based BM solutions can be classified into SL and RL techniques. In addition, we also identified some of the open challenges that have been highlighted in the previous sections. Furthermore, we have already closed the exploration phase of selecting a suitable tool for our simulation setup. We identified a suitable simulation tool that can be used to develop required simulation capabilities of 5G NR physical and MAC layer in addition to the required ML capabilities.

4.1.2 Next steps

We have already concluded our literature review phase and have done exploration for simulation tool. The next step will be the development of 3GPP specified mmWave BM framework, which will serve us as a baseline for performance comparison at a later stage. We will then simulate some of the existing state-of-the-art SL and RL based BM solutions and compare their performance against the baseline. We will then work on the identified limitations of existing techniques and will research for performance enhancements and design our solutions for an efficient mmWave BM framework. Next phase will then be concluded with the performance evaluations of our mmWave BM solutions.

4.2 Full duplex channel estimation

4.2.1 Current status and results

We have finalized our model for mmWave massive MIMO FD systems and conducted a few simulations to analyse the deep learning-based channel estimations. Our proposed deep learning works well in estimating both SI and UE channels.

4.1.2.1 System and Channel modelling for FD mmWave massive MIMO

We consider a single-cell system comprised of one FD mmWave massive MIMO BS and K_u uplink UEs and K_d downlink UEs as depicted in Figure 5.

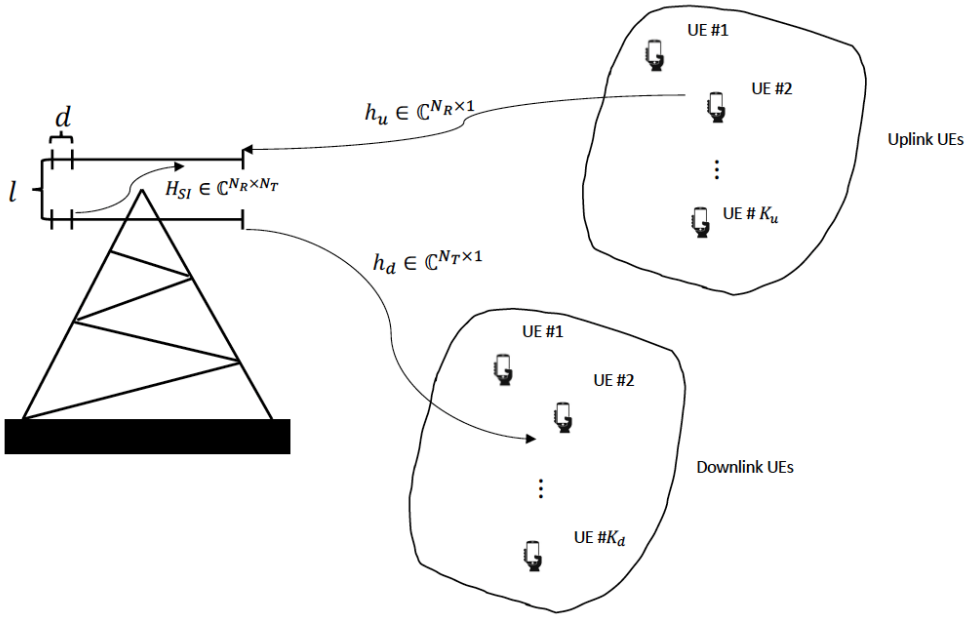

Figure 5: System model for mmWave massive MIMO FD systems.

Both uplink and downlink UEs are half-duplex devices and the total number of UEs in the cell is $K = K_u + K_d < N_T$.The number of transmit and receive antennas at BS are N_T and N_R, respectively and they are placed in a specific distance to each other, e.g., l and d is the antenna spacing.

The UE-BS channel follows a geometrical channel model as follows

$$\boldsymbol{h} = \sqrt{N_R} \sum_{i=0}^{P} \sqrt{\beta^i} \boldsymbol{a_B}(\varphi_A^i)$$

where P represents number of multi-path components, β^i stands for macro-scale fading

$$\beta^i = \zeta - 10\alpha \log(r^i) + \chi$$

where for i path, ζ denotes the average channel gain in dB at a reference distance of 1 m and specific carrier frequency, r^i is the distance between transmitter and

receiver, χ is shadow fading with standard deviation of $\boldsymbol{\sigma_{sf}}$, and α is the path loss exponent. Furthermore, $\boldsymbol{a_B}(\varphi_A^i)$ is the uniform linear array (ULA) response of receive or transmit antennas.

The SI channel is comprised of two near-field and far-field terms. The near-field term is because of closeness in placement of transmit and receive antennas while far-field term is originated from the reflection of the environment. Therefore,

$$\boldsymbol{H_{SI}} = \sqrt{\frac{\kappa}{\kappa+1}}\boldsymbol{H_{SI,NF}} + \sqrt{\frac{1}{\kappa+1}}\boldsymbol{H_{SI,FF}}$$

where κ is the Rician factor and $\boldsymbol{H_{SI,FF}}$ follows a similar formulation as UE-BS channel, but with different parameters. $\boldsymbol{H_{SI,NF}}$ channel is formulated as the following model

$$\left[\boldsymbol{H_{SI,NF}}\right]_{nm} = \frac{\rho}{r_{nm}} \exp\left(-2\pi j \frac{r_{nm}}{\lambda}\right),$$

r_{nm} is the distance between *n*-th receive antennas and *m*-th transmit antennas and ρ is a constant and λ is wavelength.

To estimate UEs-BS and SI channels, UEs and transmit antennas at BS will send pilot signals to the receive antenna at BS. Therefore, the received pilot signal at these antenna arrays will be

$$\boldsymbol{Y_p} = \sum_{i=1}^{K} \boldsymbol{h_i x_{p_i}} + \boldsymbol{H_{SI}} \mathbf{F} \boldsymbol{X_p} + \mathbf{N}.$$

Here, $\boldsymbol{Y_p} \in \mathbb{C}^{\boldsymbol{N_R} \times \boldsymbol{T}}$ is the received pilot signal at receive antennas of BS during $\boldsymbol{T}$ pilot transmissions, $\boldsymbol{x_{p_i}} \in \mathbb{C}^{\mathbf{1}\times\mathbf{1}}$ is the transmitted pilot signal from $\boldsymbol{i}$-th UE, $\boldsymbol{X_p} \in \mathbb{C}^{\boldsymbol{T}\times\boldsymbol{T}}$ is a diagonal matrix, whose diagonal elements are transmitted pilot signals from transmit antennas at BS, and $\mathbf{F} \in \mathbb{C}^{\boldsymbol{N_T}\times\boldsymbol{T}}$ is the precoding matrix of transmit antennas of BS. To reduce the pilot overhead, we propose to share resources between transmit antennas and UEs.

4.1.2.2 Pilot transmission schemes

In this section, we propose different pilot transmissions schemes for both SI and UE-BS channel estimation to reduce the high pilot overhead of FD transmissions. Typically, we need $K + \boldsymbol{N_T}$ time/frequency pilot resources to estimate SI and UE-BS channels, and compared to the half-duplex systems, $\boldsymbol{N_T}$ more resources will be consumed in FD systems, which is quite high because of the large number of antennas in mmWave massive MIMO. In order to reduce the pilot overhead, the pilot resources can be shared between transmit antennas

and UEs, but then UEs and transmit antennas would create interference to each other, which is quite similar to pilot contamination problem in massive MIMO systems. For this purpose, three different pilot transmission schemes are assumed, and they are depicted in Figure 6.

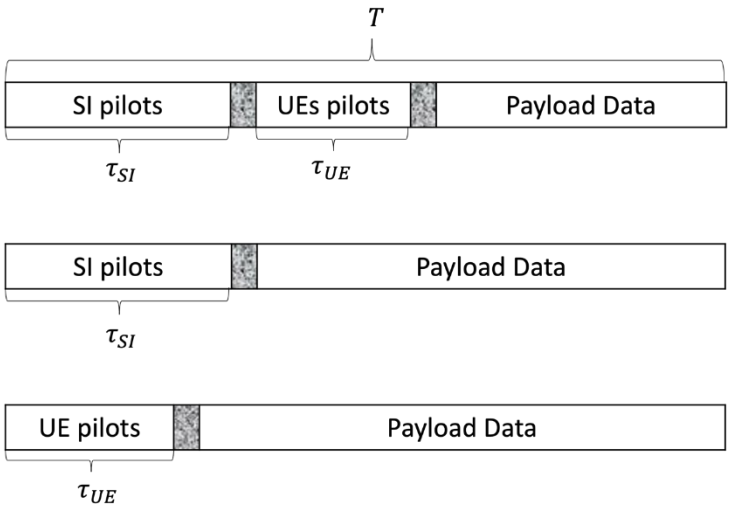

Figure 6: Pilot transmission schemes.

In the first scheme, UEs and transmit antennas of BS will transmit their orthogonal pilots at different resource (time/subcarriers) block. Therefore, there would not be any interference between pilots of transmit antennas and UEs, but pilot overhead would be extremely high. While in the second scheme, we will assume the available resource blocks for pilot transmission is equal to the number of transmit antennas at BS and UEs will reuse the same resource for their channel estimation. Pilot overhead in this scheme would be still high as the number of transmit antennas are usually large compared to the number of UEs.

In third scheme, we assume the available pilot resources will be same as the number of UEs ($\boldsymbol{K}$), and transmit antennas at BS will reuse the same resources for their channel estimation.

In this section, we dig into the channel estimation problem for both SI and UE-BS channels. Since it is expected that SI has a stronger channel compared to UEs' channels (even after propagation and analogue suppression) the first step would be estimating SI channel in the presence of UEs' pilot signals. Then after digital domain SI channel suppression, UE-BS channel will be estimated. This is a more challenging problem compared to half-duplex systems where the SI does not exist. We analyse the channel estimation problem for different pilot transmission schemes that was introduced in the previous section using deep learning.

4.1.2.3 Simulation results

In this section, we evaluate the performance of proposed DNN for different pilot transmission scenarios that were introduced in the previous section. Number of both transmit and receive antennas are 16 and they are half-wavelength uniform linear arrays and the distance between the arrays is $l = 10\lambda$. The operating frequency is 28 GHz and transmitted power of BS and UE is 30 dBm and 20 dBm, respectively. The noise variance is -174 dBm $+10\log(BW) + 10$ dB, where $BW = 400$ MHz is the bandwidth. The number of path loss components, path loss exponent and variance of shadow fading are 10, 3.1 and 8.1, respectively. Rician factor for SI channel is 30 dB and the total propagation and analogue domain SI suppression is -40 dB. We assume that the angle of arrival to the BS has a limited angular spread with uniform distribution within the interval $[-\frac{\pi}{3}, \frac{\pi}{3}]$, while the angle of departure from the transmit antenna of BS follows a uniform distribution within the interval $[-\pi, \pi]$.

The DNN is trained on Python 3.7.3 and implemented using the Keras libraries with a TensorFlow backend in the Jupyter Notebook environment. We employ Adam optimizer to update the network parameters with the learning rate of 0.001 and a batch size of 512 for 100 epochs. A summary of the architecture and number of parameters of the trained neural network is shown in Figure 7.

Layer (type)	Output Shape	Param #
input_2 (InputLayer)	(None, 16, 16, 2)	0
conv2d_5 (Conv2D)	(None, 16, 16, 4)	76
batch_normalization_5 (Batch	(None, 16, 16, 4)	16
activation_5 (Activation)	(None, 16, 16, 4)	0
conv2d_6 (Conv2D)	(None, 16, 16, 8)	296
batch_normalization_6 (Batch	(None, 16, 16, 8)	32
activation_6 (Activation)	(None, 16, 16, 8)	0
conv2d_7 (Conv2D)	(None, 16, 16, 2)	146
batch_normalization_7 (Batch	(None, 16, 16, 2)	8
activation_7 (Activation)	(None, 16, 16, 2)	0

Total params: 574
Trainable params: 546
Non-trainable params: 28

Figure 7: The architecture and number of parameters of the trained neural network.

A dataset of size 50000 samples is collected based on the considered system model and it is split into 20000, 20000, 10000 for train, validation, and test,

respectively. The validation data is used to determine that our model has not rather memorized training data and has learned some meaningful aspects of the data so that the model can be later used for prediction. Figure 8, Figure 9, and Figure 10 show the training and validation loss for different pilot transmission schemes that were introduced in previous sections. Th figures confirm that the trained neural network has learned to map the revived pilot signal to the SI channel estimates, even in the challenging scenarios where UEs create interference to the received pilot signal from the transmit antenna of BS. It is also clear that the trained neural network does not suffer from the over fitting problem, and it can predict the unseen data very well.

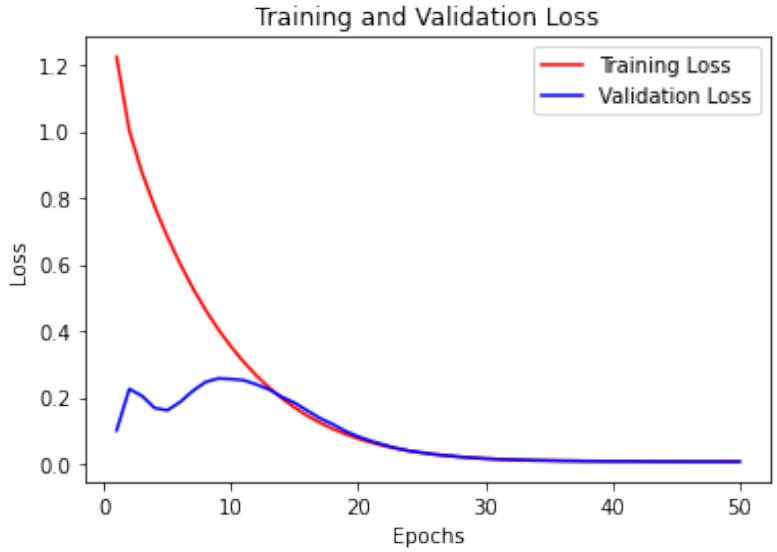

Figure 8: Training and validation loss for case 1.

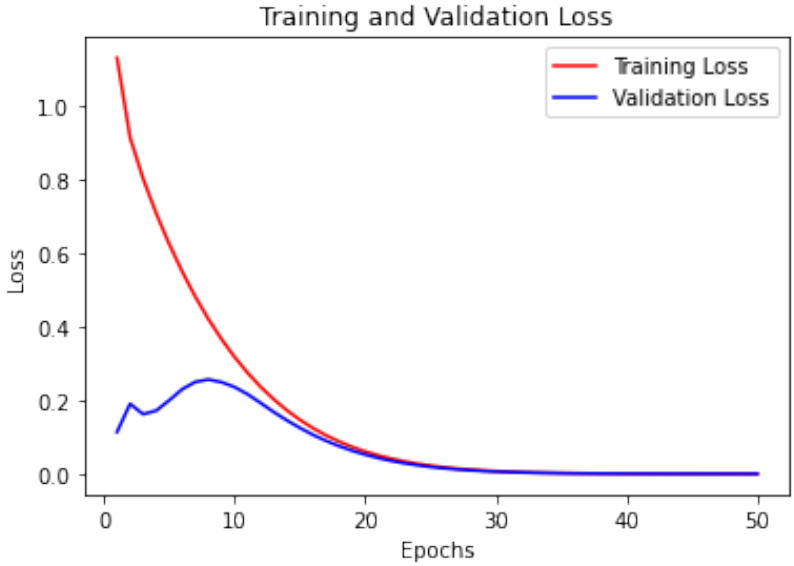

Figure 9: Training and validation loss for case 2.

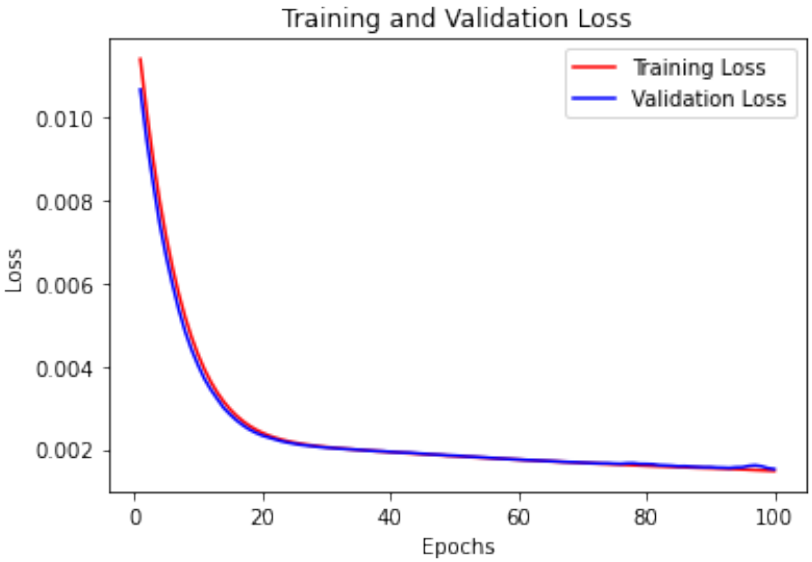

Figure 10: Training and validation loss for case 3.

4.2.2 Next steps

For the next steps, we are aimed to finalize our simulation results for a journal publication. We are also trying to provide a mathematical analysis for the effect of SI cancellations before the base band. The other interesting next step would be mapping channels between receive antenna array and transmit antenna arrays at FD BS.

4.3 Integrated access and backhaul in 5G and Beyond

In this section, a summary of the current research progress and next steps. Here, we would like to mention that the UoA-1 ESR joined the SEMANTIC project in May 2022.

4.3.1 Current status and results (early phase, emphasis on SoA)

IAB deployments can accomplish superior cell edge coverage and significantly reduce the amount of required fiber. Using more donor nodes can enhance throughput, but it can increase the amount of required fiber. On the other hand, using fewer donor nodes increases hops from IAB nodes to donor nodes and degrades the throughput and latency performance. Optimal value of donor nodes number that achieves required throughput and latency performance is an important key in IAB network. We are investigating in a novel recursive algorithm to provide the optimum resource allocations which guarantee the edge coverage and fair backhauling for all the nodes in IAB network. The main steps for the new algorithm are:

- First phase: The IAB-nodes collect all the information for each of their children node such as load, capacity and channel quality and send them to a central control unit.
- Second phase: Define the favoured downstream nodes, such as children nodes which will be served with the highest priority by their parent nodes in the spanning tree, where each parent node works to find the best solution according to its available resources.
- Third phase: Formulate the connectivity matrix among the nodes which could be formulated based on the distance, received power or other parameters for determining if there is a connection between 2 IAB nodes or not.
- Fourth phase: The central control unit determines all potential paths and solutions (Space States) to cover the downstream nodes based on the available network parameters such as IAB nodes' load, and available capacity in the links or in mediator and donor nodes, and maximum number of the hops.
- Fifth phase: The algorithm will choose the optimal paths and solutions that guarantee the nodes load offloading or even the network load balancing. That leads to determine the best network topology which guarantee the optimum network performance in term of (delay, power, data rate traffic control, etc).

4.3.2 Next steps

The expected future research will be extended based on the current work for the new algorithm with Mobile Edge Computing and Cloud Networking, as they showed a promising direction for cost-efficient in the communication networks. In addition, Network Function Virtualization and Software Defined Network are expected to play important roles in the future wireless networks by improving the dynamicity of cloud networks [ZKA21].

4.4 RIS-assisted NOMA for multi-QoS scenarios

In this section, we provide a summary of current progress and our aim for the next steps.

4.4.1 Current status and results

We consider an uplink transmission in a RIS-NOMA system, as shown in Figure 11, where a BS equipped with single-antenna receives information signals from RIS with N elements, multiple jammers with M antennas, and 2 K single antenna users using PD-NOMA. The SIC is implemented at the receiver of the BS. In the first step, the receiver decodes the signal of the near user that has a

better channel condition, then subtracts it from the received signal to decode the signal of the far user [IZD17].

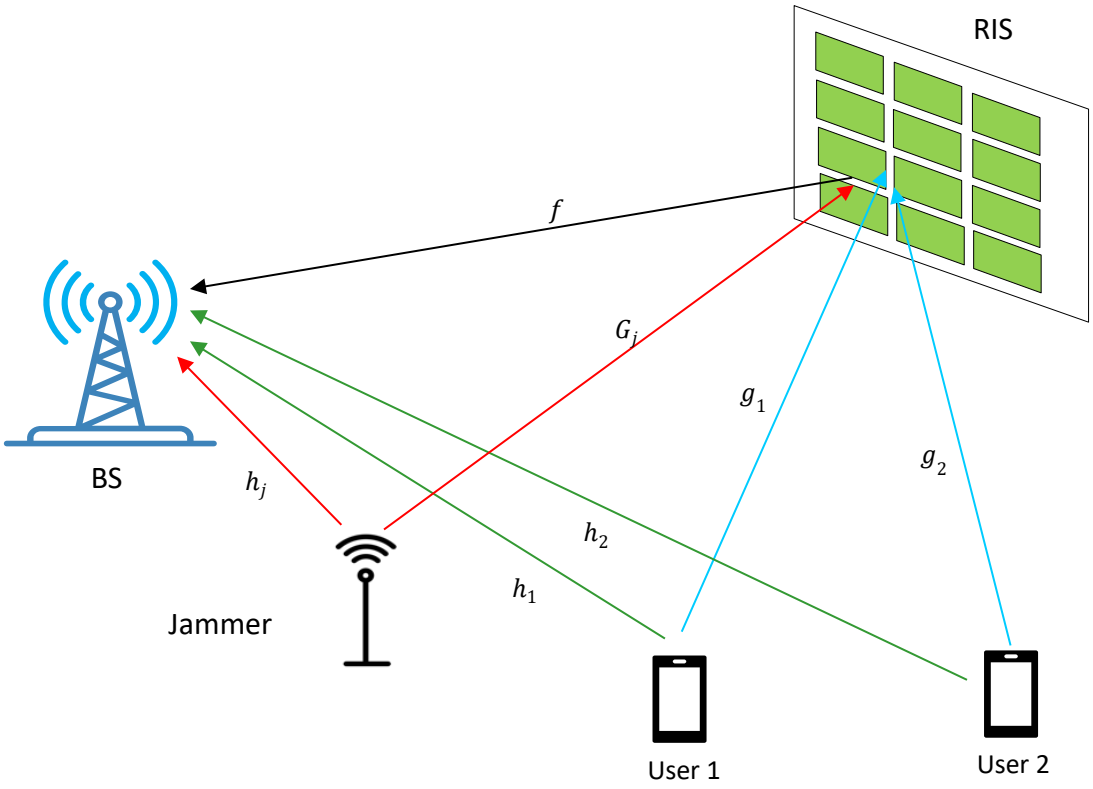

Figure 11: Illustration of RIS-NOMA aided two users uplink communication

In this section, we explain the differences between conventional non-absorptive RIS and hybrid absorptive RIS. The overall response of the RIS element can be expressed as $\phi = \beta e^{j\theta}$. Unlike a conventional non-absorptive RIS, which can only adjust the phase of the reflecting element that is fixed with $\beta = 1$, a hybrid RIS can also adjust its modulus by absorbing part of the energy of the impinging signal, i.e. the modulus coefficient of the RIS element is adjustable with $\beta = [0,1]$ or $\beta \leq 1$.

Our aim is to minimize the total power transmitted by the user terminals under quality-of-service constraints by controlling the propagation from the users to the base station with help of the RIS. The objective function and constraints are both non-linear and non-convex in our optimization problem. Our numerical results, as

shown in Figure 12, show that RIS can help to dramatically reduce the required user transmit power in an interference limited scenario.

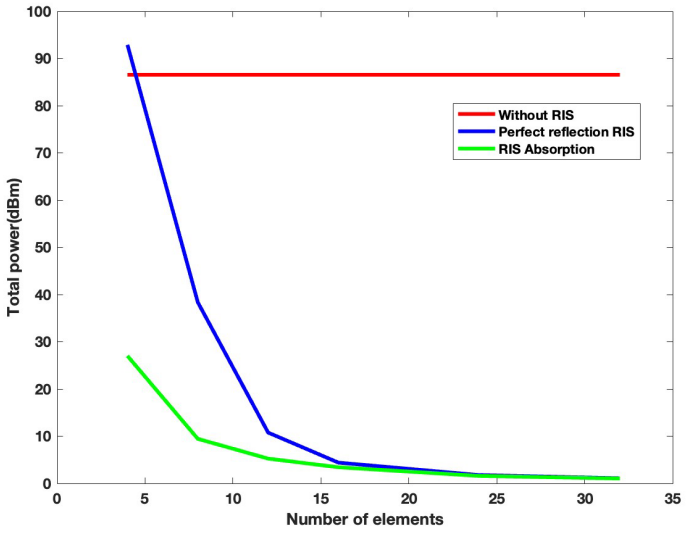

Figure 12: Required total transmit power to meet the user quality of service requirements in the presence of a jammer with M=4 antennas, as a function of number of RIS elements.

4.4.2 Next steps

Our next aim is to extend our system model and use different toolbox for solving our problem formulation. A conference publication is currently under preparation.

5 Conclusions

In this deliverable we have reported on the progress of the SEMANTIC ESR contributions towards the objectives of WP1 (Spectrum and Forward-Compatibility Aspects for multi-GHz NR operation).

Key findings and preliminary performance evaluation results on beam-based transmissions in multi-GHz bands; low-complexity techniques for channel estimation in massive MIMO in the mmWave band; distributed MIMO with focus on IAB; and NOMA for enhancing user experience in beyond 5G systems were reported.

6 References

[AAF+20] I. Aykin, B. Akgun, M. Feng and M. Krunz, “MAMBA: A Multi-armed Bandit Framework for Beam Tracking in Millimeter-wave Systems,” in *IEEE INFOCOM 2020 - IEEE Conference on Computer Communications*, 2020.

[AHS+22] D. Adesina, C.-C. Hsieh, Y. E. Sagduyu and L. Qian, “Adversarial Machine Learning in Wireless Communications using RF Data: A Review,” *IEEE Communications Surveys & Tutorials*, no. 1-1, 2022.

[APD+14] A. Sabharwal, P. Schniter, D. Guo, D. W. Bliss, S. Rangarajan and R. Wichman, "In-Band Full-Duplex Wireless: Challenges and Opportunities," in *IEEE Journal on Selected Areas in Communications*, vol. 32, no. 9, pp. 1637-1652, Sept. 2014, doi: 10.1109/JSAC.2014.2330193.

[AT17] A. Masmoudi and T. Le-Ngoc, "Channel estimation and self-interference cancelation in full-duplex communication systems," in *IEEE Transactions on Vehicular Technology*, vol. 66, no. 1, pp. 321-334, Jan. 2017, doi: 10.1109/TVT.2016.2540538.

[BAD+12] B. P. Day, A. R. Margetts, D. W. Bliss and P. Schniter, "Full-Duplex Bidirectional MIMO: Achievable Rates Under Limited Dynamic Range," in *IEEE Transactions on Signal Processing*, vol. 60, no. 7, pp. 3702-3713, July 2012, doi: 10.1109/TSP.2012.2192925.

[BDE+19] Bana, A. S., De Carvalho, E., Soret, B., Abrao, T., Marinello, J. C., Larsson, E. G., & Popovski, P. ”Massive MIMO for internet of things (IoT) connectivity,” *Physical Communication*, vol. 37, p. 100859, December 2019.

[CGG+21] M. Cudak, A. Ghosh, A. Ghosh and J. Andrews, "Integrated Access and Backhaul: A Key Enabler for 5G Millimeter-Wave Deployments," in *IEEE Communications Magazine*, vol. 59, no. 4, pp. 88-94, April 2021, doi: 10.1109/MCOM.001.2000690.

[DA22] U. Demirhan and A. Alkhateeb, Integrated sensing and communication for 6G: Ten key machine learning roles, *arXiv preprint* arXiv:2208.02157, 2022.

[DAM19] D. Burgha, N. A. A. and A. F. Molisch, “A Machine Learning Solution for Beam Tracking in mmWave Systems,” in *2019 53rd Asilomar Conference on Signals, Systems, and Computers*, 2019.

[DLM+14] D. Korpi, L. Anttila and M. Valkama, "Impact of received signal on self-interference channel estimation and achievable rates in in-band

full-duplex transceivers," *2014 48th Asilomar Conference on Signals, Systems and Computers*, 2014, pp. 975-982, doi: 10.1109/ACSSC.2014.7094599.

[DSL+17] B. Di, L. Song, Y. Li and Z. Han, "V2X Meets NOMA: Non-Orthogonal Multiple Access for 5G-Enabled Vehicular Networks," in *IEEE Wireless Communications*, vol. 24, no. 6, pp. 14-21, Dec. 2017.

[DTM+15] D. Korpi, T. Riihonen and M. Valkama, "Achievable rate regions and self-interference channel estimation in hybrid full-duplex/half-duplex radio links," *2015 49th Annual Conference on Information Sciences and Systems (CISS)*, 2015, pp. 1-6, doi: 10.1109/CISS.2015.7086821.

[DWD+18] L. Dai, B. Wang, Z. Ding, Z. Wang, S. Chen and L. Hanzo, ”A Survey of Non-Orthogonal Multiple Access for 5G,” in *IEEE Communications Surveys & Tutorials*, vol. 20, no. 3, pp. 2294-2323, 2018.

[EAS+14] E. Everett, A. Sahai and A. Sabharwal, "Passive Self-Interference Suppression for Full-Duplex Infrastructure Nodes," in *IEEE Transactions on Wireless Communications*, vol. 13, no. 2, pp. 680-694, February 2014, doi: 10.1109/TWC.2013.010214.130226.

[ECB+21] H. Echigo, Y. Cao, M. Bouazizi and T. Ohtsuki, “A Deep Learning-Based Low Overhead Beam Selection in mmWave Communications,” *IEEE Transactions on Vehicular Technology,* vol. 70, no. 1, pp. 682-691, 2021.

[FRA+14] F. Boccardi, R. W. Heath, A. Lozano, T. L. Marzetta and P. Popovski, "Five disruptive technology directions for 5G," in *IEEE Communications Magazine*, vol. 52, no. 2, pp. 74-80, February 2014, doi: 10.1109/MCOM.2014.6736746.

[GLS20] R. Gupta, K. Lakshmanan and A. K. Sah, “Beam Alignment for mmWave Using Non-Stationary Bandits,” *IEEE Communications Letters,* vol. 24, no. 11, pp. 2619-2622, 2020.

[GPR+19] M. Giordani, M. Polese, A. Roy, D. Castor and M. Zorzi, “A Tutorial on Beam Management for 3GPP NR at mmWave Frequencies,” *IEEE Communications Surveys & Tutorials*, vol. 21, no. 1, pp. 173-196, 2019.

[GWL+19] Y. Guo, Z. Wang, M. Li and Q. Liu, “Machine Learning Based mmWave Channel Tracking in Vehicular Scenario,” in *2019 IEEE International Conference on Communications Workshops (ICC Workshops)*, 2019.

[HA+21] Y. Heng and J. G. Andrews, “Machine Learning-Assisted Beam Alignment for mmWave Systems,” *IEEE Transactions on Cognitive Communications and Networking,* vol. 7, no. 4, pp. 1142-1155, 2021.

[HCN+21] S. Hu, X. Chen, W. Ni, E. Hossain and X. Wang, “Distributed Machine Learning for Wireless Communication Networks: Techniques, Architectures, and Applications,” *IEEE Communications Surveys & Tutorials*, vol. 23, no. 3, pp. 1458-1493, 2021.

[HHZ+20] J. hang, Y. Huang, Y. Zhou and X. You, “Beam Alignment and Tracking for Millimeter Wave Communications via Bandit Learning,” *IEEE Transactions on Communications,* vol. 68, no. 9, pp. 5519-5533, 2020.

[HKS18] M. Hashemi, C. E. Koksal and N. B. Shroff, “Out-of-Band Millimeter Wave Beamforming and Communications to Achieve Low Latency and High Energy Efficiency in 5G Systems,” *IEEE Transactions on Communications,* vol. 66, no. 2, pp. 875-888, 2018.

[HMA21] Y. Heng, J. Mo and J. G. Andrews, “Learning Probing Beams for Fast mmWave Beam Alignment,” in *2021 IEEE Global Communications Conference (GLOBECOM)*, 2021.

[HSK+18] M. Hashemi, A. Sabharwal, C. Emre Koksal and N. B. Shroff, “Efficient Beam Alignment in Millimeter Wave Systems Using Contextual Bandits,” in *IEEE INFOCOM 2018 - IEEE Conference on Computer Communications*, 2018.

[IAD+16] S. M. R. Islam, N. Avazov, O. A. Dobre and K. -s. Kwak, ” Power-domain non-orthogonal multiple access (NOMA) in 5G systems: Potentials and challenges.,” *IEEE Communications Surveys & Tutorials*, vol. 19, no. 2, pp. 721-742, 2016.

[IZD17] Islam, S. M., Zeng, M., & Dobre, O. A., “NOMA in 5G systems: Exciting possibilities for enhancing spectral efficiency,” *IEEE 5G Tech Focus*, vol. 1, p. 2, 2017.

[KKI+21] J. Kaur, M. A. Khan, M. Iftikhar, M. Imran and Q. Emad Ul Haq, “Machine Learning Techniques for 5G and Beyond,” *IEEE Access*, vol. 9, pp. 23472-23488, 2021.

[KLA21] A. A. Khan, A. A. Laghari and S. A. Awan, “Machine learning in computer vision: A review,” *EAI Endorsed Transactions on Scalable Information Systems*, vol. 8, no. 32, pp. e4-e4, 2021.

[LFT+15] L. Wang, F. Tian, T. Svensson, D. Feng, M. Song and S. Li, "Exploiting full duplex for device-to-device communications in

heterogeneous networks," in *IEEE Communications Magazine*, vol. 53, no. 5, pp. 146-152, May 2015, doi: 10.1109/MCOM.2015.7105653. Systems and Computers, 2014, pp. 975-982, doi: 10.1109/ACSSC.2014.7094599.

[LJH+21] I. P. Roberts, J. G. Andrews, H. B. Jain and S. Vishwanath, "Millimeter-Wave Full Duplex Radios: New Challenges and Techniques," in *IEEE Wireless Communications*, vol. 28, no. 1, pp. 36-43, February 2021, doi: 10.1109/MWC.001.2000221.

[LLM+21] Liu, Y., Liu, X., Mu, X., Hou, T., Xu, J., Di Renzo, M., & Al-Dhahir, N. (2021). Reconfigurable intelligent surfaces: Principles and opportunities. *IEEE communications surveys & tutorials*, 23(3), 1546-1577.

[LVV+20] A. Łukowa, V. Venkatasubramanian, E. Visotsky and M. Cudak, "On the Coverage Extension of 5G Millimeter Wave Deployments Using Integrated Access and Backhaul," *2020 IEEE 31st Annual International Symposium on Personal, Indoor and Mobile Radio Communications*, 2020, pp. 1-7, doi: 10.1109/PIMRC48278.2020.9217260.

[LWS20] J. Y. Lai, W. -H. Wu and Y. T. Su, "Resource Allocation and Node Placement in Multi-Hop Heterogeneous Integrated-Access-and-Backhaul Networks," in *IEEE Access*, vol. 8, pp. 122937-122958, 2020.

[MBP+22] J. Morais, A. Behboodi, H. Pezeshki and A. Alkhateeb, “Position Aided Beam Prediction in the Real World: How Useful GPS Locations Actually Are?”, *arXiv preprint* arXiv:2205.09054}, 2022.

[MMF+20] C. Madapatha, B. Makki, C. Fang, O. Teyeb, E. Dahlman, M.-S. Alouini, and T. Svensson, “Integrated access and backhaul networks: Current status and potentials,” *IEEE Open Journal of the Communications Society*, 2020.

[MSW21] K. ,. H. D. Ma, H. Sun and Z. Wang, “Deep Learning Assisted mmWave Beam Prediction with Prior Low-frequency Information},” in *ICC 2021 - IEEE International Conference on Communications*, 2021.

[MZW20] K. Ma, P. Zhao and Z. wang, “Deep Learning Assisted Beam Prediction Using Out-of-Band Information,” in *2020 IEEE 91st Vehicular Technology Conference (VTC2020-Spring)*, 2020.

[PRM21] M. Polese, F. Restuccia and T. Melodia, “DeepBeam: Deep waveform learning for coordination-free beam management in mmWave networks,” in *Proceedings of the Twenty-second International*

Symposium on Theory, Algorithmic Foundations, and Protocol Design for Mobile Networks and Mobile Computing, 2021.

[PRM+21] M. Polese, F. Restuccia and T. Melodia, “Dataset for DeepBeam,” [Online]. Available: https://repository.library.northeastern.edu/collections/neu:ww72bh952.

[PZP+22] M. Pagin, T. Zugno, M. Polese and M. Zorzi, "Resource Management for 5G NR Integrated Access and Backhaul: A Semi-Centralized Approach," in *IEEE Transactions on Wireless Communications*, vol. 21, no. 2, pp. 753-767, Feb. 2022.

[RMC20] S. Rezaie, C. N. Manchón and E. de Carvalho, “Location- and Orientation-Aided Millimeter Wave Beam Selection Using Deep Learning,” in *ICC 2020 - 2020 IEEE International Conference on Communications (ICC)*, 2020.

[RPM+21] L. Rao, M. Pant, L. Malviya, A. Parmar and S. V. Charhate, “5G beamforming techniques for the coverage of intended directions in modern wireless communication: in-depth review,” *International Journal of Microwave and Wireless Technologies*, vol. 13, no. 10, pp. 1039-1062, 2021.

[SAD18] C. Saha, M. Afshang, and Harpreet S. Dhillon “Bandwidth Partitioning and Downlink Analysis in mmWave Integrated Access and Backhaul for 5G,” *IEEE Transactions on Wireless Communications*, 2018.

[SCW+19] B. P. S. Sahoo, C. -C. Chou, C. -W. Weng and H. -Y. Wei, "Enabling Millimeter-Wave 5G Networks for Massive IoT Applications: A Closer Look at the Issues Impacting Millimeter-Waves in Consumer Devices Under the 5G Framework," in *IEEE Consumer Electronics Magazine*, vol. 8, no. 1, pp. 49-54, Jan. 2019.

[SD19] C. Saha and H. Dhillon, "Millimeter wave integrated access and backhaul in 5G: Performance analysis and design insights", *IEEE J. Sel. Areas Commun.*, vol. 37, no. 12, pp. 2669-2684, Dec. 2019.

[SGM17] A. Sharma, R. K. Ganti and J. K. Milleth, "Joint backhaul-access analysis of full duplex self-backhauling heterogeneous networks", *IEEE Trans. Wireless Commun.*, vol. 16, no. 3, pp. 1727-1740, Mar. 2017.

[SKA+21] S. Sarkar, M. Krunz, I. Aykin and D. Manzi, “Machine Learning for Robust Beam Tracking in Mobile Millimeter-Wave Systems,” in *2021 IEEE Global Communications Conference (GLOBECOM)*, 2021.

[SKG+15] S. Singh, M. N. Kulkarni, A. Ghosh, and J. G. Andrews, “Tractable model for rate in self-backhauled millimeter wave cellular networks,” *IEEE J. Sel. Areas Commun.*, vol. 33, no. 10, pp. 2196–2211, 2015.

[SLP+20] M. S. Sim, Y.-G. Lim, S. H. Park, L. Dai and C.-B. Chae, “Deep Learning-Based mmWave Beam Selection for 5G NR/6G With Sub-6 GHz Channel Information: Algorithms and Prototype Validation,” *IEEE Access,* vol. 8, pp. 51634-51646, 2020.

[SMO+19] S. M. Riazul Islam, Ming Zeng, Octavia A. Dobre, Kyung-Sup Kwak, ”Non orthogonal multiple access (NOMA): How it meets 5g and beyond,” *Wiley 5G Ref: The Essential 5G Reference* Online, pp. 1-28, 2019.

[SZS18] Sadia, H., M. Zeeshan, and S.A. Sheikh, “Performance analysis of downlink power domain NOMA under fading channels,” in *2018 ELEKTRO*, 2018.

[TG17] E. Turgut and M. C. Gursoy, "Coverage in heterogeneous downlink millimeter wave cellular networks", *IEEE Trans. Commun.*, vol. 65, no. 10, pp. 4463-4477, Oct. 2017.

[TJ91] Thomas M. Cover, Joy A, Elements of information theory, *College of New York*, 1991.

[TSM+21] H. Tataria, M. Shafi, A. F. Molisch, M. Dohler, H. Sjoland, and F. Tufvesson, “6G wireless systems: Vision, requirements, challenges, insights, and opportunities,” *Proceedings of the IEEE*, vol. 109, no. 7, pp. 1166–1199, 2021.

[VCS+18] V. Va, J. Choi, T. Shimizu, G. Bansal and R. W. Heath, “Inverse Multipath Fingerprinting for Millimeter Wave V2I Beam Alignment,” *IEEE Transactions on Vehicular Technology,* vol. 67, no. 5, pp. 4042-4058, 2018.

[VSB+17] V. Va, T. Shimizu, G. Bansal and R. W. Heath, “Position-aided millimeter wave V2I beam alignment: A learning-to-rank approach,” in *2017 IEEE 28th Annual International Symposium on Personal, Indoor, and Mobile Radio Communications (PIMRC)*, 2017.

[WCW+18] J.-B. Wang, M. Cheng, J.-Y. Wang, M. Lin, Y. Wu, H. Zhu and J. Wang, “Bandit inspired beam searching scheme for mmWave high-speed train communications,” *arXiv preprint* arXiv:1810.06150, 2018.

[WKR+19] Y. Wang, A. Klautau, M. Ribero, A. C. K. Soong and R. W. Heath, “MmWave Vehicular Beam Selection With Situational Awareness Using Machine Learning,” *IEEE Access,* vol. 7, pp. 87479-87493, 2019.

[WNH18] Y. Wang, M. Narasimha and R. W. Heath, “mmWave Beam Prediction with Situational Awareness: A Machine Learning Approach,” in *2018 IEEE 19th International Workshop on Signal Processing Advances in Wireless Communications (SPAWC)*, 2018.

[WOZ+19] R. Wang, O. Onireti, L. Zhang, M. A. Imran, G. Ren, J. Qiu and T. Tian, “Reinforcement Learning Method for Beam Management in Millimeter-Wave Networks,” in *2019 UK/ China Emerging Technologies (UCET)*, 2019.

[XXT+16] X. Xiong, X. Wang, T. Riihonen and X. You, "Channel estimation for full-duplex relay systems with large-scale antenna arrays," in *IEEE Transactions on Wireless Communications*, vol. 15, no. 10, pp. 6925-6938, Oct. 2016, doi: 10.1109/TWC.2016.2593729.

[XZC+20] H. Xiao, X. Zhang, A. T. Chronopoulos, Z. Zhang, H. Liu and S. Ouyang, "Resource Management for Multi-User-Centric V2X Communication in Dynamic Virtual-Cell-Based Ultra-Dense Networks," in *IEEE Transactions on Communications*, vol. 68, no. 10, pp. 6346-6358, Oct. 2020.

[YXL+21] Yang, G., Xu, X., Liang, Y. C., & Di Renzo, M. (2021). Reconfigurable intelligent surface-assisted non-orthogonal multiple access. *IEEE Transactions on Wireless Communications*, 20(5), 3137-3151.

[YYA+13] Y. Saito, Y. Kishiyama, A. Benjebbour, T. Nakamura, A. Li and K. Higuchi, "Non-Orthogonal Multiple Access (NOMA) for Cellular Future Radio Access," *2013 IEEE 77th Vehicular Technology Conference (VTC Spring)*, 2013, pp. 1-5, doi: 10.1109/VTCSpring.2013.6692652.

[ZHW+21] J. Zhang, Y. Huang, J. Wang, X. You and C. Masouros, “Intelligent Interactive Beam Training for Millimeter Wave Communications,” *IEEE Transactions on Wireless Communications,* vol. 20, no. 3, pp. 2034-2048, 2021.

[ZKA21] Y. Zhang, M. A. Kishk, and M.-S. Alouini, “A survey on integrated access and backhaul networks,” *Front. Comms. Net.*, vol. 2, Jun. 2021.

[ZKA21] Y. Zhang, M. Kishk and S. Alouini, "Computation Offloading and Service Caching in Heterogeneous MEC Wireless Networks," in *IEEE Transactions on Mobile Computing*, doi: 10.1109/TMC.2021

[ZPX+17] Z. Xiao, P. Xia and X. -G. Xia, "Full-Duplex Millimeter-Wave Communication," in *IEEE Wireless Communications*, vol. 24, no. 6, pp. 136-143, Dec. 2017.

[ZXK+15] Z. Zhang, X. Chai, K. Long, A. V. Vasilakos and L. Hanzo, "Full duplex techniques for 5G networks: self-interference cancellation, protocol design, and relay selection," in *IEEE Communications Magazine*, vol. 53, no. 5, pp. 128-137, May 2015.

[ZZM+17] Z. Zhang, Z. Chen, M. Shen, B. Xia, W. Xie and Y. Zhao, "Performance Analysis for Training-Based Multipair Two-Way Full-Duplex Relaying With Massive Antennas," in *IEEE Transactions on Vehicular Technology*, vol. 66, no. 7, pp. 6130-6145, July 2017.